ADA041596

RADC-TR-77-210
Final Technical Report
June 1977

MILLIMETER WAVE GYROTRON DEVELOPMENT - PHASE I

Varian Associates, Inc.

Sponsored by
Defense Advanced Research Projects Agency (DoD)
ARPA Order No. C192

DDC
JUL 15 1977
C

Approved for public release; distribution unlimted.

The views and conclusions contained in this document are those of the
authors and should not be interpreted as necessarily representing the
official policies, either expressed or implied, of the Defense
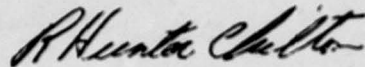Advanced Research Projects Agency or the U. S. Government.

AD No.
DDC FILE COPY

ROME AIR DEVELOPMENT CENTER
Air Force Systems Command
Griffiss Air Force Base, New York   13441

This report has been reviewed by the RADC Information Office (OI) and is releasable to the National Technical Information Service (NTIS). At NTIS it will be releasable to the general public, including foreign nations.

This report has been reviewed and is approved for publication.

APPROVED: *R Hunter Chilton*

R. HUNTER CHILTON
Project Engineer

Do not return this copy. Retain or destroy.

MILLIMETER WAVE GRYOTRON DEVELOPMENT - PHASE I

Howard R. Jory

SECURITY CLASSIFICATION OF THIS PAGE *(When Data Entered)*

REPORT DOCUMENTATION PAGE		READ INSTRUCTIONS BEFORE COMPLETING FORM
1. REPORT NUMBER RADC-TR-77-210	**2. GOVT ACCESSION NO.**	**3. RECIPIENT'S CATALOG NUMBER**
4. TITLE *(and Subtitle)* MILLIMETER WAVE GYROTRON DEVELOPMENT - PHASE I		**5. TYPE OF REPORT & PERIOD COVERED** Final Technical Report 25 Mar 76 - 30 Apr 77
		6. PERFORMING ORG. REPORT NUMBER N/A
7. AUTHOR(s) Howard R. Jory		**8. CONTRACT OR GRANT NUMBER(s)** F30602-76-C-0237 ARPA Order-C192
9. PERFORMING ORGANIZATION NAME AND ADDRESS Varian Associates, Inc. 611 Hansen Way Palo Alto CA 94303		**10. PROGRAM ELEMENT, PROJECT, TASK AREA & WORK UNIT NUMBERS** 62301E C1920002
11. CONTROLLING OFFICE NAME AND ADDRESS Defense Advanced Research Projects Agency 1400 Wilson Blvd Arlington VA 22209		**12. REPORT DATE** June 1977
		13. NUMBER OF PAGES 68
14. MONITORING AGENCY NAME & ADDRESS *(if different from Controlling Office)* Rome Air Development Center (OCTP) Griffiss AFB NY 13441		**15. SECURITY CLASS.** *(of this report)* UNCLASSIFIED
		15a. DECLASSIFICATION/DOWNGRADING SCHEDULE N/A

16. DISTRIBUTION STATEMENT *(of this Report)*

Approved for public release; distribution unlimited.

17. DISTRIBUTION STATEMENT *(of the abstract entered in Block 20, if different from Report)*
Same

18. SUPPLEMENTARY NOTES
RADC Project Engineer:
R. Hunter Chilton (OCTP)

19. KEY WORDS *(Continue on reverse side if necessary and identify by block number)*
Gyrotron, Gryoklystron, C-band oscillations, TE mode propagation, cyclotron resonance maser, cyclotron harmonic operation, millimeter wave amplifier, computer-simulated beam performance.

20. ABSTRACT *(Continue on reverse side if necessary and identify by block number)*
This report describes Phase I of a program to develop a high-power 94 GHz amplifier based on the gyrotron or cyclotron resonance interaction. Ultimate goals are 100 kw peak power, 5 to 10 kW average power, 1 to 10% bandwidth, 30% beam efficiency, and 30 dB gain. The experimental work in Phase I has been performed at X-band to demonstrate feasibility of this approach. The first section of this report contains a review of previous work on cyclotron resonance devices. This is followed by the analysis of a number of cyclotron harmonic interactions with TE_{01} and TE_{n1} cylindrical fields. The next

DD FORM 1473 **1 JAN 73** EDITION OF 1 NOV 65 IS OBSOLETE

SECURITY CLASSIFICATION OF THIS PAGE *(When Data Entered)*

section describes the design of an X-band gyroklystron amplifier. A calculation of large-signal power output is included which predicts an efficiency from beam power to microwave output of 36%. A computer simulation of the gun and beam performance is presented. Initial measured results for the experimental amplifier are presented. The maximum measured gain was 9 - 10 dB. The gain was limited by an interfering oscillation which prevented full optimization of the beam parameters. One oscillation produced an output power of 19.5 kw peak with an efficiency of |9.8%. An analysis is included to predict the bandwidth of gyroklystrons at 94 GHz. Bandwidths of 1 to 4% are predicted with the fundamental interaction which requires a super-conducting magnet. Significantly reduced bandwidths result when cyclotron harmonic interactions are used to allow room-temperature magnets. It is concluded that the basic feasibility of the gyroklystron amplifier has been demonstrated. Future effort should include modifications to improve stability, gain, and bandwidth, further exploration of high cyclotron harmonic operation, and investigation of traveling wave interactions.

TABLE OF CONTENTS

LIST OF ILLUSTRATIONS

LIST OF ILLUSTRATIONS (Cont.)

(The reverse of this page is blank)

I. INTRODUCTION

This report describes Phase I of a program to develop a high-power 94 GHz amplifier. Tentative specification goals are 100 kw peak power, 5 to 10 kW average power, 1 to 10% bandwidth, 30% beam efficiency, and 30 dB gain.

The decision was made at the start of Phase I to pursue the development of a new type of amplifier based on the gyrotron, or cyclotron resonance maser, interaction in order to accomplish these goals. The advantages of this interaction are that beam and circuit dimensions can be large compared to a wavelength.

Phase I of this development program had the specific goals of (1) calculating the strength of the gyrotron interactions with various cavity modes and various cyclotron harmonics and (2) the design and construction and initial test of an experimental amplifier operating at 10.35 GHz to demonstrate the feasibility of the gyrotron as a 94 GHz amplifier. The 10.35 GHz amplifier was designed to have full power output, gain, and efficiency, but reduced percentage bandwidth.

The gyrotrons reported in the Russian literature have all been single-cavity oscillators. Calculations for multi-cavity amplifiers can be found in the literature, but some of the practical problems relating to stability are not discussed and no experimental results are presented. The 10.35 GHz feasibility tube was designed to operate as a three-cavity amplifier with 26 dB gain. It therefore represents a significant advance in the state of the art.

The first section of this report contains a review of previous work on gyrotrons or cyclotron resonance devices. This is followed by the analysis of a number of cyclotron harmonic interactions with TE_{01} and TE_{n1} cylindrical fields. These calculations led to the selection of TE_{011} cavities operating at the second harmonic of the cyclotron frequency for use in the X-band experimental gyroklystron.

The next section describes the design of the X-band gyroklystron. A calculation of large-signal power output is included which employed a ballistic trajectory

1

code. The calculation predicted an efficiency from beam power to microwave output of 36%. A computer simulation of the gun and beam performance is presented, and the design and shaping of the magnetic field is discussed.

Initial measured results for the experimental amplifier are presented. The maximum measured gain was 9 - 10 dB. The gain was limited by an interfering oscillation which prevented full optimization of the beam parameters. A discussion is included of the oscillations observed as magnetic field was varied. One of these oscillations produced an output power of 19.5 kw peak with an efficiency of 9.8%. It involved an interaction at the second harmonic of the cyclotron frequency with an output cavity resonance different than the design resonance.

An analysis is included to predict the bandwidth of gyroklystrons at 94 GHz. Bandwidths of 1 to 4% are predicted with the fundamental interaction which requires a superconducting magnet. Significantly reduced bandwidths result when cyclotron harmonic interactions are used to allow room-temperature magnets.

It is concluded that the basic feasibility of the gyroklystron amplifier has been demonstrated. Future effort should include modifications to improve stability, gain, and bandwidth, further exploration of high cyclotron harmonic operation, and investigation of traveling wave interactions. These are discussed further in the final section.

II. REVIEW OF PREVIOUS WORK ON GYROTRONS

Amplifiers and oscillators based on the principles of cyclotron resonance have been the subject of investigations spread over a considerable time period. We will not present a complete listing of references on this subject, but will discuss several that are representative.

A cyclotron resonance device in which the electron motion was determined by crossed dc electric and magnetic fields was described by Swift-Hook and Reddish[1]. An oscillator based on cyclotron resonance with dc magnetic field was built by Chow and Pantell[2]. A discussion of cyclotron devices from the point of view of maser action was presented by Hirshfield and Wachtel[3]. An oscillator which produced watt power levels at millimeter wavelengths was reported by Bott[4]. Similar results with related devices were presented by Beasley[5]. The Hirshfield, Bott, and Beasley devices all used corkscrew magnetic fields to produce transverse electron velocity followed by magnetic adiabatic compression of the beam. The millimeter devices used superconducting solenoids.

Work on X-band cyclotron wave devices was done by Schriever and Johnson[6] at the University of Utah. This work resulted in a traveling wave device which could operate either as an amplifier or an oscillator. Measured gain as high as 20 dB was achieved and power output as an oscillator was 720 W at X-band. Another X-band oscillator using a short cavity resonator was reported by Kulke and Wilmarth[7].

Recent work by Granatstein[8,9] has dealt with cyclotron resonance effects with very high peak power, short pulse, electron beams. Power levels of 50 Mw peak at 8 GHz were obtained, for example, with a beam voltage of about 1 MV and useful beam current of about 1500 A, for an efficiency of 3%. Pulse lengths were of the order of 50 nsec and pulsing was nonrepetitive. Peak power of the order of 2 MW in the 60 to 90 GHz range has also been obtained with similar beams where the output frequency is a high multiple of the cyclotron frequency. A gain of 16 dB was also demonstrated in a traveling wave amplifier using a relativistic beam.

The record for high cw power near 100 GHz reported in the literature at this time appears to be 10 kW cw at 2.78 mm wavelength. This was reported by Zaytsev et al[10]. This power was obtained with a cyclotron resonance oscillator (gyrotron) using the fundamental cyclotron frequency interaction. Because this is a significantly higher power level than achieved by other approaches, we will discuss this work in more detail. The configuration of the device is indicated in Figure 1. The interaction uses a hollow cylindrical electron beam where individual electrons have helical motion. The microwave structure is a cylindrical TE_{021} resonator with a fairly large length-to-diameter ratio. (Actual dimensions are not given in the reference.)

Beam parameters are reported to be 27 kV and 1.4 A, and the electron axial velocity was given as 2/3 of the rotational velocity. For 27 kV, the total electron velocity is 0.315 c (where c is the velocity of light) and the rotational velocity v_t is 0.262 c. The measured efficiency was 31% for the conversion of beam power to microwave output power.

In the gyrotron interaction, it is clear that energy exchange between the electrons and the microwave fields occurs by virtue of an E_ϕ field in the local coordinate system for the orbiting electron. For the TE_{02} interaction, the local E_ϕ field is also the E_ϕ field in the cavity coordinate system. For maximum interaction with the fundamental cyclotron resonance, all electrons should be located in a region where the cavity E_ϕ has a maximum value.

Operation of a gyrotron oscillator using the second harmonic of the cyclotron frequency was also reported by Zaytsev[10]. The configuration of the device was essentially the same as that for the fundamental gyrotron shown in Figure 1 except that the TE_{231} and TE_{031} cylindrical cavity modes were used instead of the TE_{021}. The reported efficiency of the harmonic oscillator was significantly lower. The maximum reported value was 15%.

Another very impressive gyrotron oscillator employing second harmonic operation has been reported by Kisel' et al[11]. The device indicated in Figure 2 was similar

4

1 - Solenoid
2 - Cryostat
3 - Injector
4 - Resonator
5 - Collector
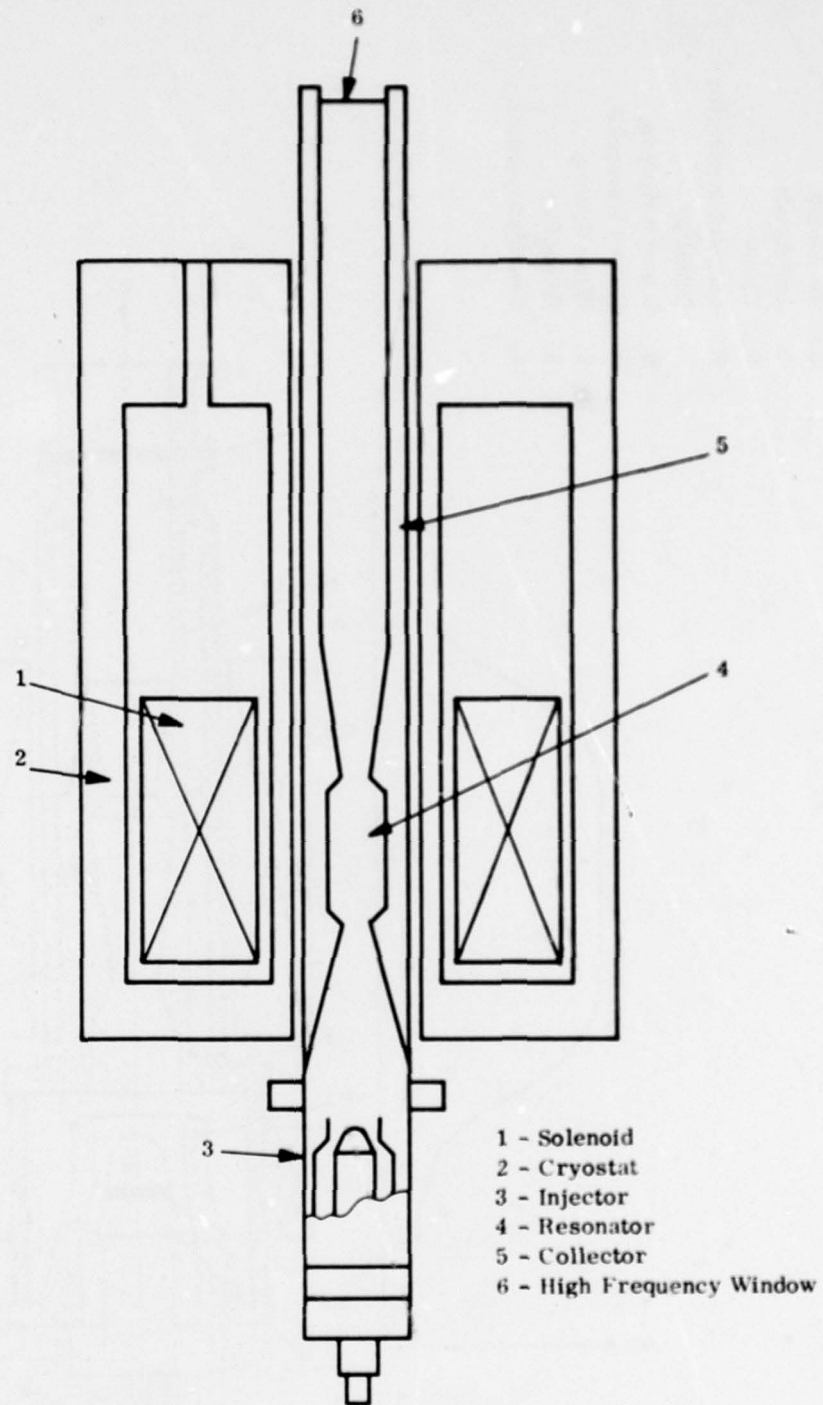6 - High Frequency Window

Figure 1. Gyrotron Configuration (after Zaytsev)

1. Gun Structure
2. Emitting Area
3. 1st Anode
4. 2nd Anode
5. Cavity
6. Output Coupling Iris
7. Collector
8. Vacuum Window
9. Output Waveguide
10,12. Water Cooling
11,13. Solenoids
14. Ceramic Insulators
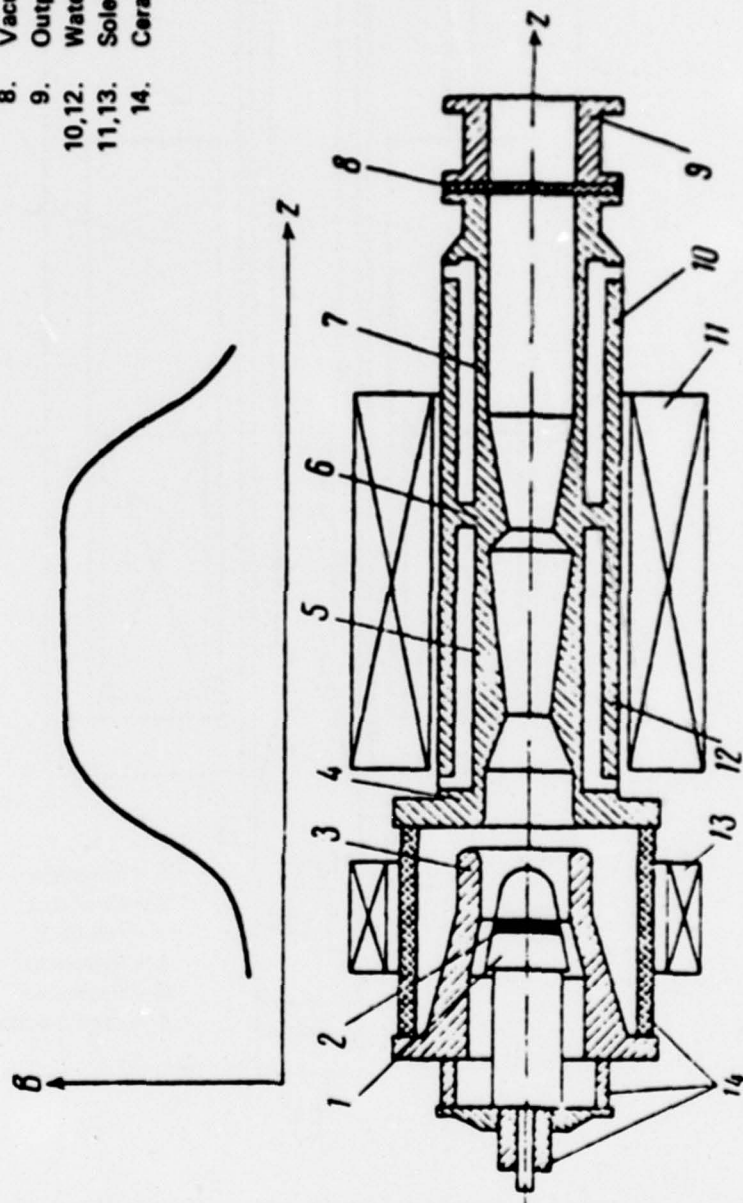
Figure 2. Drawing of Experimental Gyrotron and the Axial Distribution of the Magnetic Field (after Kisel')

to the one built by Zaytsev, except that a room-temperature solenoid was used. A power output of 10 kW cw at 8.9 mm wavelength was obtained with an efficiency of 40%. With pulsed operation, the output was 30 kW at 43% efficiency.

The excellent efficiency of this device was attributed to the use of special shaping techniques for the microwave field in the oscillator cavity. The essential feature of the field shaping apparently is to apply lower electric field in the beginning of the cavity where electron bunching is taking place and higher field later when energy is being removed from the bunched beam. The field shaping is accomplished by varying the cavity diameter. The cavity shaping is indicated in Figure 2, which shows the cross section of the experimental oscillator.

Another approach for cyclotron resonance devices is to employ a beam in which each electron orbits about a nearly common axis. Then one can employ a circularly-polarized cavity mode, for which all electrons see essentially the same average component of E_ϕ. The disadvantage of this approach is that for low beam voltages the useful beam area is relatively small. In practice, the useful beam area is limited to a thin ring having a diameter equal to the orbit diameter. This disadvantage is minimized by going to high voltage beams where the orbit radius becomes large.

This approach of orbiting electrons around the cavity axis also allows relatively strong interactions to occur at high harmonics of the cyclotron frequency. An experimental device using harmonics up to the 13th harmonic was demonstrated by Jory[12]. This device was based on interaction with TE_{n11} cylindrical fields. Measured efficiencies in the high harmonic device were 1% or less.

The excellent efficiencies reported by Zaytsev and by Kisel' make it particularly promising to build on that technology. A key feature is the electron gun approach which uses a geometry similar to the magnetron injection gun. The generation of a beam with small velocity spread is clearly of the utmost importance to achieve high efficiency.

(The reverse of this page is blank)

7

III. ANALYSIS OF CYCLOTRON HARMONIC INTERACTIONS

A. BALLISTIC TRAJECTORY ANALYSIS CODE

Several years ago, a proprietary computer code was developed at Varian to calculate the motion of charged particles in electromagnetic fields with an applied dc magnetic field[13].

The relativistic force equation for a particle having mass m, charge q, position r, and velocity v in an electric field E and magnetic field B is (mks units)

$$(d/dt) \left[m \vec{v}(\vec{r}, t) \right] = \left[\vec{E}(\vec{r}, t) + \vec{v}(\vec{r}, t) \times \vec{B}(\vec{r}, t) \right] \quad . \tag{1}$$

By writing the relativistic mass in terms of rest mass and velocity

$$m = m_o / (1 - v^2/c^2)^{1/2} \quad , \tag{2}$$

and by performing considerable algebraic manipulation, we can put Equation 1 into the following form:

$$(d/dt) \, \vec{v}(\vec{r}, t) = (q/\gamma m_o) \left\{ \vec{E}(\vec{r}, t) + \vec{v}(\vec{r}, t) \times \vec{B}(\vec{r}, t) - \left[\vec{v}(\vec{r}, t)/c^2 \right] \right.$$
$$\left. \left[\vec{v}(\vec{r}, t) \cdot \vec{E}(\vec{r}, t) \right] \right\} \quad . \tag{3}$$

This form is more convenient for numerical integration.

The rest mass is denoted by m_o and the relativistic factor $1/(1 - v^2/c^2)^{1/2}$ is denoted by γ. The position of the particle is given by $\vec{r}$, where

$$(d/dt) \, \vec{r} = \vec{v}(\vec{r}, t) \quad . \tag{4}$$

The code operates by performing a numerical time-stepping integration of Equation 3 in rectangular coordinates. The time step is typically chosen to be small enough that the error per step is less than one part in 10^6. The code is designed to

9

use either TE or TM cylindrical waveguide or cavity fields. All E and B components for the particular mode being considered are included in the calculation.

In addition to the electromagnetic fields, a static dc magnetic field can be included in the calculation in the form

$$B_r = -B_0 \, \alpha \, I_1 \, (2\pi \, r/L) \sin \, (2\pi \, z/L) \tag{5}$$

$$B_z = B_0 \, 1 - \alpha I_0 \, (2\pi \, r/L) \cos \, (2\pi \, z/L) \quad ; \tag{6}$$

where I_0 and I_1 are modified Bessel functions, α is an amplitude parameter, and L is a length parameter. These parameters can be chosen to apply a magnetic mirror field with mirrors located at $z = \pm L/2$, and with a mirror ratio, $R_m = (1+\alpha)/(1-\alpha)$. Or, with $\alpha = 0$, a uniform dc magnetic field is applied.

This code can be used to calculate the motion of electrons through a gyrotron cavity including all cavity field components, all relativistic effects, and any nonlinear effects in the motion. It is, of course, necessary to specify an amplitude for the cavity fields which is consistent with the cavity loaded Q and the energy transferred from the electrons moving through the cavity. Therefore, to simulate an interaction involving specified beam and cavity parameters where nonlinear effects exist, it will in general require iterations on the assumed field amplitude until a self-consistent calculation is obtained.

A limitation on the code is that it does not include space-charge effects. This does not appear to be a serious limitation for gyrotron devices.

B.   NORMALIZATION OF ELECTRIC FIELD AMPLITUDE

To make comparisons between harmonic interactions with various waveguide or cavity modes, the trajectory code was used to calculate the change in energy for electrons injected into the microwave fields for an arbitrary number of microwave cycles. The calculations were made with sufficiently small microwave field amplitudes

10

so that small-signal conditions apply and the change in energy is linearly related to the amplitude of the electric field.

For simplicity in the calculations, the electrons are injected at the center of a cavity, with respect to the axial coordinate, where the transverse electric field has a maximum value, and the axial velocity of the electron is taken to be zero so that the electrons remain in the central axial plane. In a real device the electrons would enter from the end of the cavity and experience a sinusoidal variation in electric field amplitude in traveling through the cavity. They would also encounter microwave magnetic field components near the ends of the cavity. For the interactions of interest, the microwave magnetic fields have only a small effect. Also, for typical gyrotron beams where the transverse velocity is large compared to the axial velocity, the transit time effects are important only to the extent that they determine the total time the fields are applied to a given electron. In typical gyrotron interactions, the total transit time is 10 cycles or more. The calculations with electrons restricted to the central axial plane save considerable computation time, and are valid provided the above assumptions are met.

To compare various interactions, curves will be plotted of the peak values of the sinusoidal energy modulation of the electrons for various orbit positions, cyclotron harmonics, and cavity modes. In comparing cases where different cavity modes are involved, a problem arises as to how the results should be normalized. The most reasonable normalization appears to be to evaluate $\Delta V / E \lambda N \beta_\perp$ where ΔV is the peak energy modulation, E is the peak electric field, λ is wavelength, N is total number of microwave cycles in the calculation, and $\beta_t = v_t/c$ where v_t is the transverse electron velocity. The denominator $E \lambda N \beta_t$ is the product of electric field times path length for the electron. In the case of TE_{011} cylindrical cavities, the electric field value to use in the normalization is clearly E_ϕ, since this is the only component present. For other cavity modes such as the TE_{n11} cylindrical modes, the choice is not clear because both E_ϕ and E_r are present. Still other alternatives

11

for normalization would be to relate ΔV in some way to total stored energy in the cavity or to loss power density in the cavity walls.

For the TE_{n11} resonator the cavity fields are given by:

$$H_z = AJ_n (k_c r) \cos (\beta Z) \begin{cases} \cos n\phi \\ \sin n\phi \end{cases} \tag{7}$$

$$E_z = 0 \tag{8}$$

$$E_r = jA \frac{n}{k_c r} \sqrt{\mu/\epsilon} \frac{f}{f_c} J_n (k_c r) \cos (\beta Z) \begin{cases} \sin n\phi \\ -\cos n\phi \end{cases} \tag{9}$$

$$E_\phi = jA \sqrt{\mu/\epsilon} \frac{f}{f_c} J'_n (k_c r) \cos (\beta Z) \begin{cases} \cos n\phi \\ \sin n\phi \end{cases} \tag{10}$$

$$H_r = A \frac{f}{f_c} \sqrt{1 - \left(\frac{f_c}{f}\right)^2} J'_n (k_c r) \sin (\beta Z) \begin{cases} \cos n\phi \\ \sin n\phi \end{cases} \tag{11}$$

$$H_\phi = A \frac{n}{k_c r} \frac{f}{f_c} \sqrt{1 - \left(\frac{f_c}{f}\right)^2} J_n (k_c r) \sin (\beta Z) \begin{cases} -\sin n\phi \\ \cos n\phi \end{cases} \tag{12}$$

where $J_n (k_c r)$ is a Bessel function of the first kind of order n, k_c is the cutoff wave number defined by $k_c = 2\pi f_c/c$, f_c is the cutoff frequency, and A is an amplitude factor. The axial propagation constant, β, is defined by

$$\beta = \frac{\omega}{c} \sqrt{1 - \left(\frac{f_c}{f}\right)^2} \tag{13}$$

$J'_n (k_c r)$ indicates the derivative of J_n with respect to the argument, $k_c r$. These fields are sketched in Figure 3 for the case of n = 4. Figure 3 and Equations 9 and 10 illustrate a problem that arises in evaluating the TE_{n11} modes: both the E_r and E_ϕ fields have sinusoidal variations with angle. Also, the mode can exist in a linearly
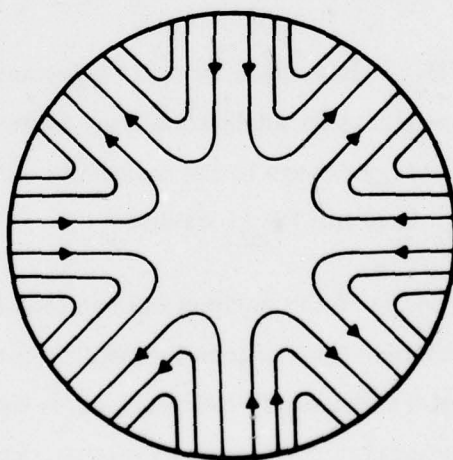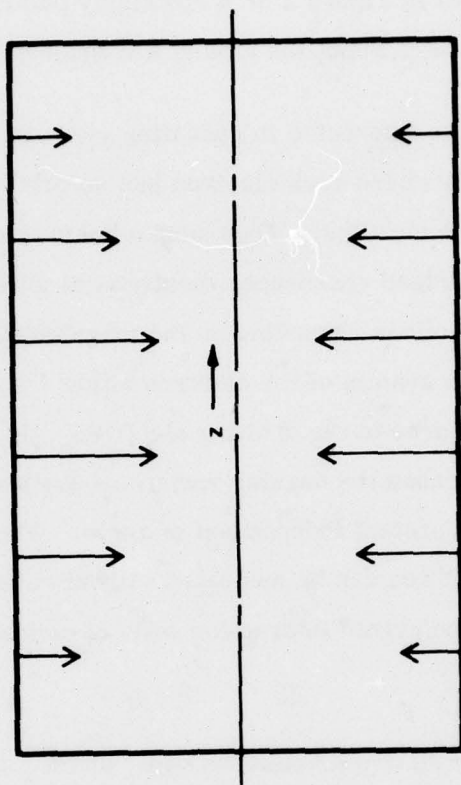
12

Figure 3. TE$_{411}$ Mode in Cylindrical Resonator

13

polarized version as shown in Figure 3 or a circularly polarized version in which the pattern of Figure 3 rotates about the axis at a frequency ω/n.

We will generally be interested in operating gyrotron devices with hollow cylindrical electron beams where each electron has an orbit radius that is small compared to the hollow beam radius. When such a beam is used for an interaction with a TE_{n11} linearly polarized resonance, electrons at different angular positions could have different interactions depending on the magnitudes of E_r and E_ϕ. Note that in the local coordinate system of the electron either the E_r or the E_ϕ cavity field can apply tangential force to the orbiting electron. Also if E_r and E_ϕ have the same magnitude, then (because the angular variations are sinusoidal) the magnitude of E, $|E| = \sqrt{E_r^2 + E_\phi^2}$ is constant independent of angle. When these conditions apply a linearly polarized interaction can be evaluated without compensating for angular variations. A circularly polarized interaction will, of course, have no angular variations in coupling factor.

An example of the relative magnitudes of E_r and E_ϕ are shown in Figure 4 for a TE_{411} cavity. One would expect interaction calculations to be independent of angle for normalized radii up to a value of 3; minor variations with angle may occur with electrons at radii from 3 to 4, and significant variations would be likely for larger radii.

In evaluating the TE_{411} interaction we will be primarily concerned with radii less than 4; hence, the dependence on angle should not be important. We have chosen to normalize the electron energy change to the maximum value of the electric field, which will always be the E_r field for TE_{n11} cavities.

All calculations to compare the various interactions use synchronous values of magnetic field. For harmonic interactions the applied magnetic field is the fundamental, relativistic, cyclotron resonance field divided by the harmonic number. The synchronous fields give the maximum energy modulation, which is the parameter being used to compare the interactions. One could also use slightly nonsynchronous
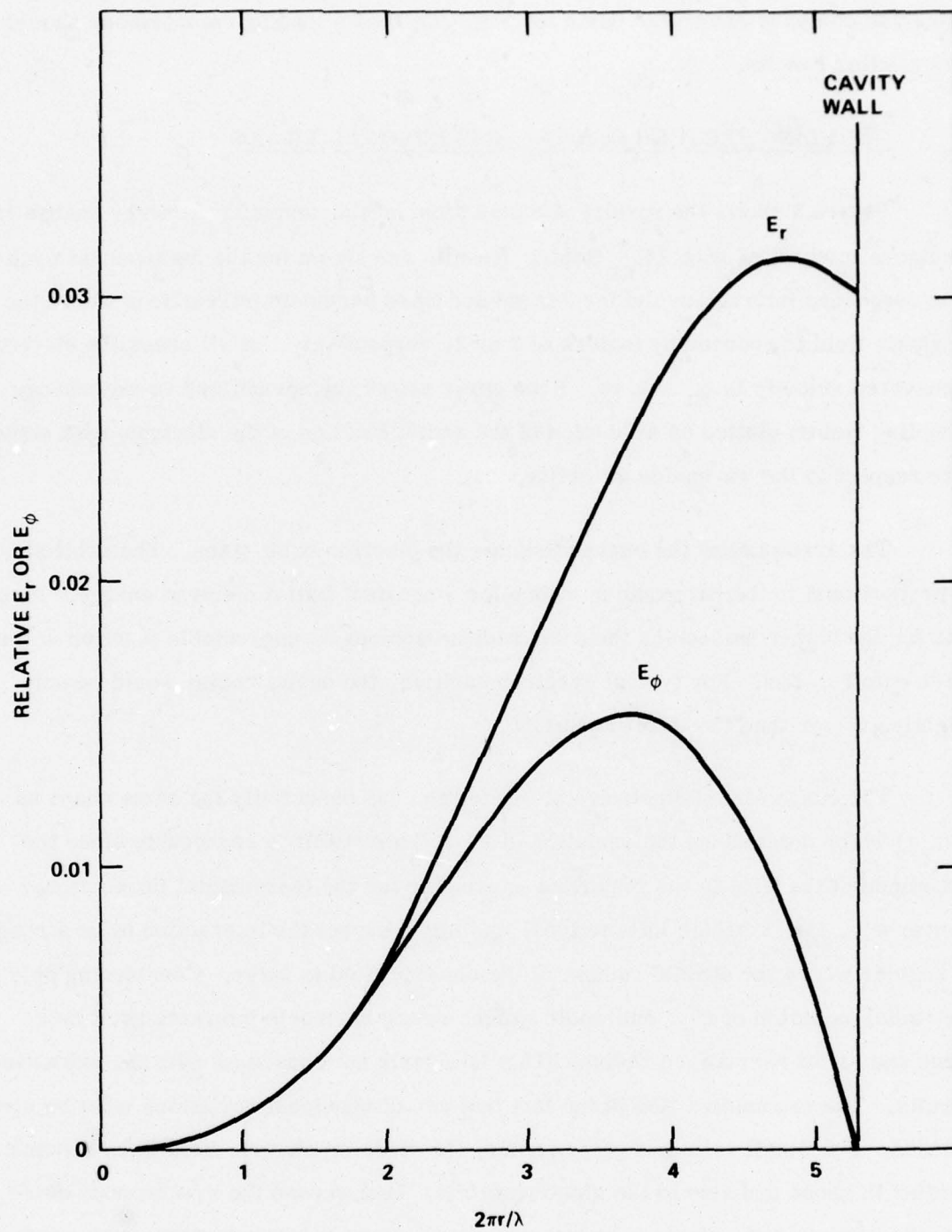
14

Figure 4. Relative Magnitudes of E_r and E_ϕ for a TE_{411} Cavity

fields and compare electronic beam loading. The beam loading comparisons should give similar results.

C.   COUPLING FACTORS FOR TE$_{01}$ CYLINDRICAL FIELDS

Figure 5 shows the results of calculations of the normalized energy change for electrons interacting with TE$_{01}$ fields. Results are shown for the fundamental cyclotron resonance interaction and for second and third harmonic interactions where the magnetic field is reduced by factors of 2 or 3, respectively. In all cases the electron transverse velocity is $v_\perp = 0.4c$. Each curve shows the normalized energy change (coupling factor) plotted as a function of the radial location of the electron orbit center with respect to the waveguide or cavity axis.

The arrows near the curves indicate the electron orbit sizes. The orbit size is proportional to the harmonic numbers for a constant initial electron energy. Note that for the higher harmonics the orbit radius becomes an appreciable function of the guide cutoff radius. For typical gyrotron cavities, the cavity radius would be only slightly greater than the cutoff radius.

The curve for the fundamental interaction has essentially the same shape as $J_1(k_c r)$ which determines the variation of E_ϕ. This result is reasonable since the magnitude of the field is the important parameter for the fundamental interaction. Conversely, for harmonic interactions, one might expect the interaction to be strong in regions where the spacial radient of the electric field is large. Considering only the radial variation of E_ϕ, one would expect strong harmonic interactions at both large and small normalized radius. This is clearly not consistent with the calculated results. The explanation lies in the fact that two dimensional variations must be considered. For small values of guide radius, the circular electric field lines become similar in shape and size to the electron orbits. In that case the synchronous component of force on the electron approaches zero. Harmonic interactions with orbits centered at $k_c r = 1.84$ are apparently reasonably strong because of the curvature effects. When the electrons are on the portion of their orbits closer to the guide axis,
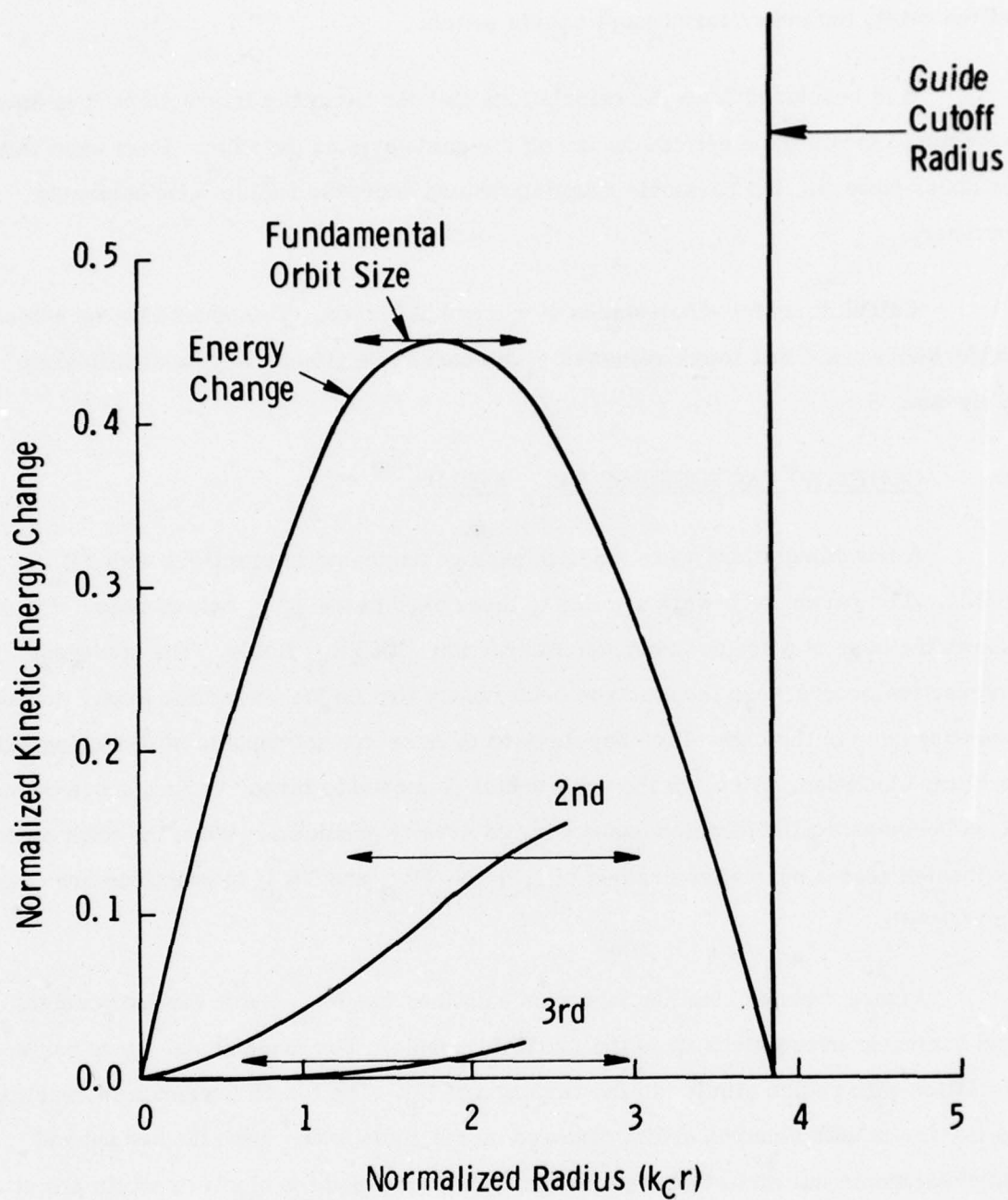
16

Figure 5. Cyclotron Harmonic Coupling Factors and Orbit
Size in TE_{01} Fields $v_t = 0.4 c$

the electron path curvature is opposite to the field curvature. During other portions of the orbit, both curvatures more nearly match.

It is concluded from the calculations that for harmonic interactions it is advantageous to locate the electrons as far off the guide axis as possible. Even when this is done, however, the harmonic coupling factors decrease rapidly with harmonic number.

Calculations for other values of v_t were not made. This should be the subject of further work. For lower values of v_t the curvature effects may be significantly different.

D.   COUPLING FACTORS FOR TE_{n1} FIELDS

A few calculations were made to explore harmonic interactions with TE_{n1} fields. The parameters were similar to those used in the TE_{01} calculations. Figure 6 shows the case of a second harmonic interaction with TE_{21} fields. The strongest interaction occurs when the electron orbit center lies on the waveguide axis. However, the guns used in the high-efficiency Russian devices are not capable of producing axis-orbiting electrons. Also, as the orbit center is moved to larger radius, more beam area becomes available which eases current density problems. When the orbit center is located near a normalized radius of 1.8, the TE_{21} and TE_{01} interactions are equal in strength.

Figure 7 shows coupling factor calculations for TE_{41} fields for fundamental and harmonic interactions up to the fourth harmonic. The fundamental curve has a variation with radius similar to the variation of E_r. The fourth harmonic interaction is maximum with electron orbits centered on the guide axis. Both the second and third harmonic interactions have maximum strength when the electron orbits are at intermediate radial positions. A somewhat surprising result is that both the second and third harmonics have reasonably good interaction with the TE_{41} fields. For the third harmonic, the TE_{41} is better than the TE_{01} interaction.

18
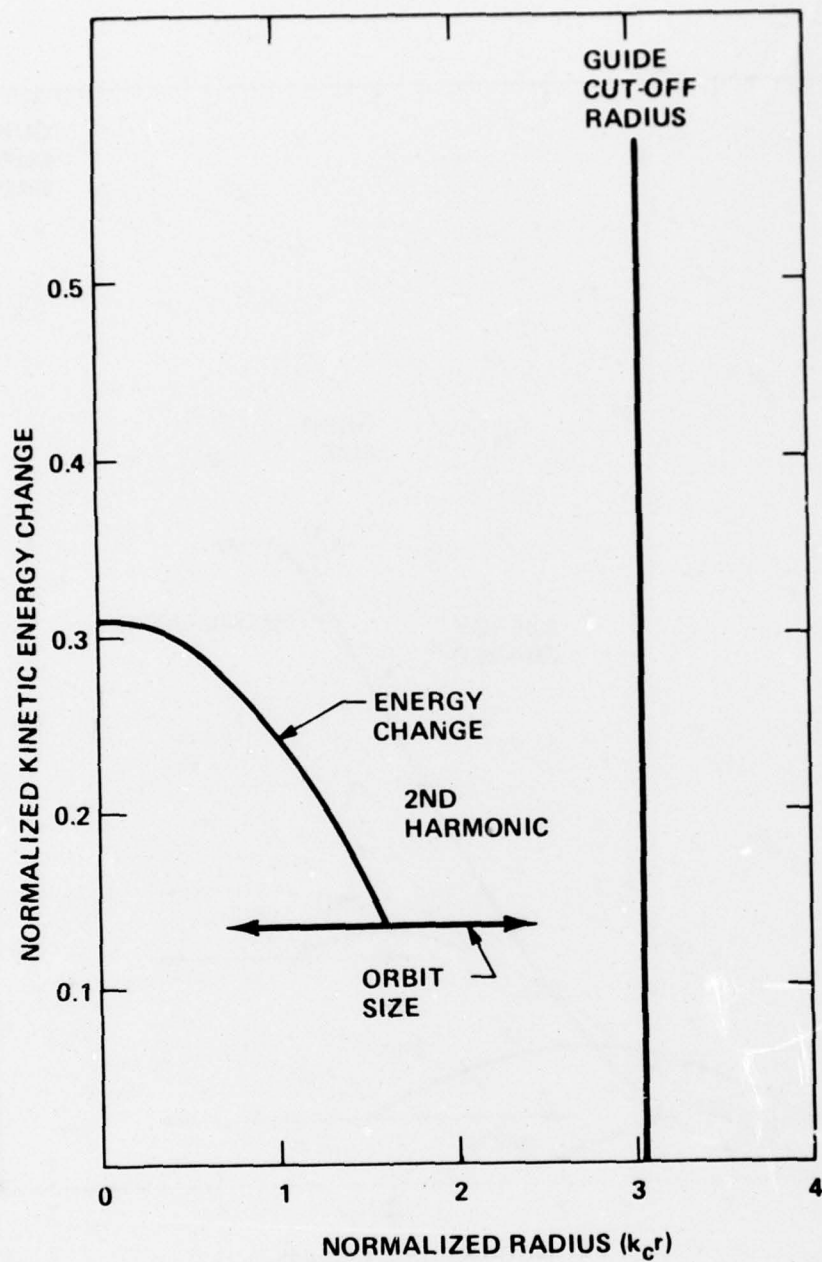
Figure 6. Second Harmonic Coupling Factor and Orbit
Size in TE$_{21}$ Fields v$_t$ = 0.4 c
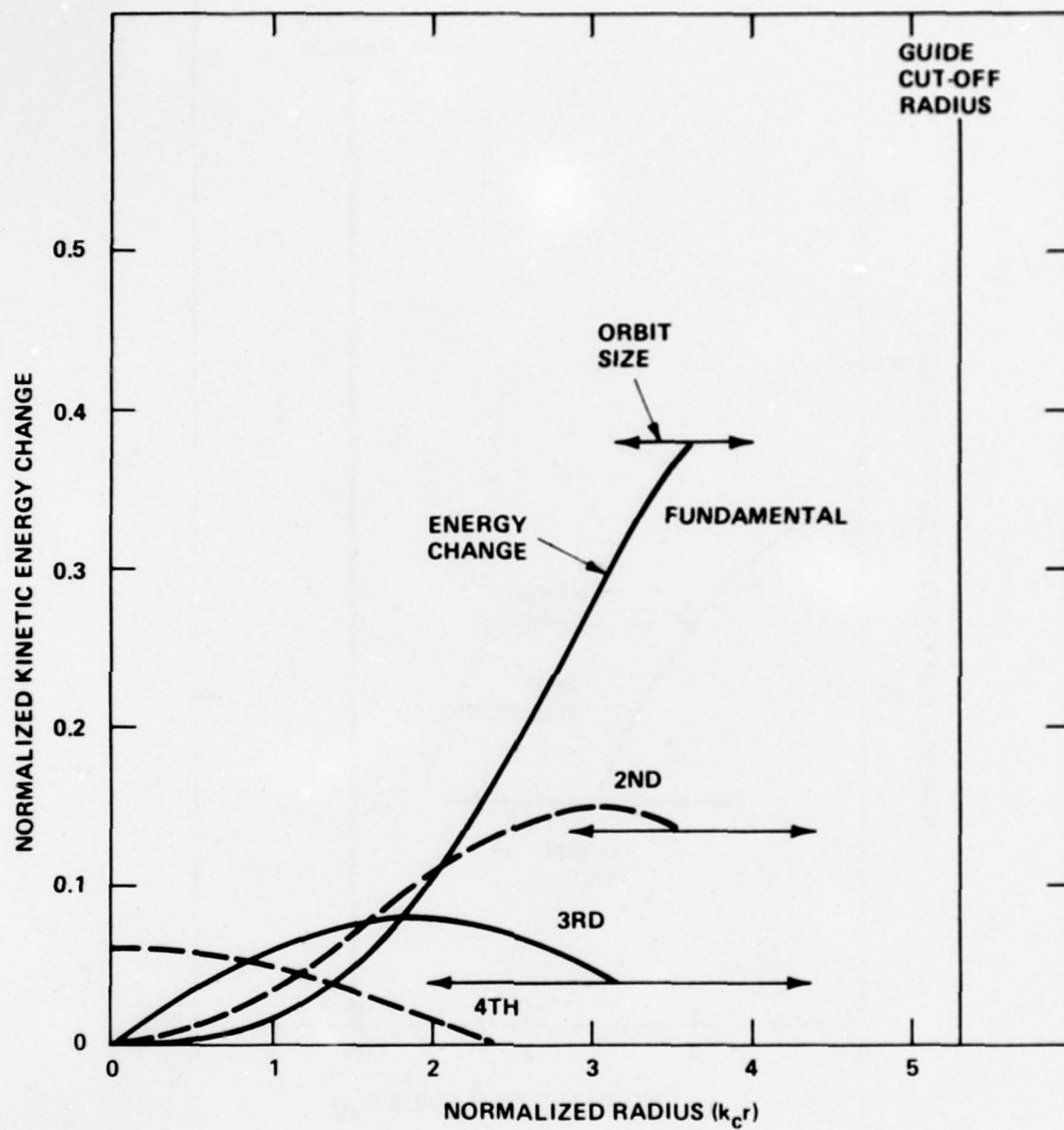
Figure 7. Cyclotron Harmonic Coupling Factors and
Orbit Size in TE_{41} Fields $v_t = 0.4$ c

20

It is recognized that the few calculations reported are not adequate to evaluate the best third and fourth harmonic interactions. The main purpose of the calculations was to determine if the TE_{01} second harmonic interaction was worth testing in an experimental device. The calculations indicate that this is a reasonable choice.

(The reverse of this page is blank)

IV. DESIGN OF AN X-BAND SECOND HARMONIC GYROKLYSTRON AMPLIFIER

A. CHOICE OF TUBE PARAMETERS

The choice of operating parameters for the experimental tube was made with a number of requirements in mind:

1. Demonstration of a high gain amplifier

2. Building on the published Russian high-efficiency devices

3. Exploration of operation at cyclotron harmonics

4. Operation at a frequency where costs would be minimum

5. Scalability of the design to 94 GHz

6. Demonstration of high-power output and efficiency

High instantaneous bandwidth, although of interest ultimately, was considered to be of secondary importance in the initial experiment.

With these considerations in mind, the choice was made to build a multicavity gyroklystron amplifier. The use of resonant cavities would enable the experimental device to have an interaction similar to the successful Russian devices. The analysis of harmonic interactions summarized in the previous section indicated that operation on the second harmonic of the cyclotron frequency with TE_{011} resonant cavities should give a reasonably strong interaction. This was also consistent with the Russian experience.

Initial choices of beam voltage and current at 60 kV and 5 A were made by assuming an efficiency of 33% and using a dc beam impedance similar to the beam impedances in the Russian devices. A transverse to axial velocity ratio of two was chosen for design purposes. The beam orbit center radius was determined as a

23

compromise between a small beam which would have a weaker interaction and a large beam which might have some interception on the drift tubes. The drift tube diameter was set at a value which would be beyond cutoff for the TE_{01} cylindrical mode at the design frequency, but would allow propagation in the TE_{21} and TE_{11} modes. The design frequency was selected to be 10.35 GHz, a frequency where drive power sources are available. This frequency results in a synchronous magnetic field for the second harmonic interaction of 2000 gauss which is easily achievable.

The lengths of the cavities in the gyroklystron amplifier were determined by efficiency, stability, and power density considerations. For high efficiency the effective voltage developed in the output cavity should be similar to the dc beam voltage. The effective voltage for a gyrotron cavity for the fundamental cyclotron resonance interaction is [17]

$$\Delta V = \frac{1}{\pi} \ E\lambda \ \frac{L}{\lambda} \ \frac{v_t}{v_z} \tag{14}$$

where L is the axial length, v_t is the transverse component of electron velocity, v_z is the axial component, and E is the peak transverse electric field in the cavity. For cyclotron harmonic interactions, we can write

$$\Delta V = \frac{1}{\pi} \ E\lambda \ \frac{L}{\lambda} \ \frac{v_t}{v_z} \ F_n \tag{15}$$

where F_n is a reduction factor relating coupling factor for the harmonic of interest to the peak coupling for the fundamental interaction. The value of F_n can be obtained from Figure 5 for TE_{01} fields.

A trial choice was made for the output cavity length of $L = 3\lambda$. Then, taking $F_n = 0.3$, $v_t = 2v_z$, and $\Delta V = 60$ kV, we get $E\lambda = 1.04 \times 10^5$. At 94 GHz with $\lambda = 3.2$ mm, the peak electric field would be 3.3×10^5 V/cm. This value of field is rather high, but it should be achievable with the TE_{01} mode where there are no E fields normal to

24

conductors. At 10.35 GHz where $\lambda = 2.9$ cm, the peak E field would be 3.6×10^4 V/cm, which is a conservative value.

To investigate the properties of an output cavity of length 3λ in more detail, the trajectory code described earlier was used. Figure 8 shows energy versus time for eight electrons passing through the cavity with the initial phase of the cavity fields stepped in increments of $\pi/4$. All electrons have the same initial velocities of $v_z = 0.2$ c and $v_t = 0.4$ c. The magnetic field for the calculation was chosen to be 6% less than the synchronous value for the second harmonic cyclotron interaction; that is, $\omega = 2 \times 1.06 \, \omega_c$, where the relativistic cyclotron frequency is

$$\omega_c = \frac{eB}{\gamma m} \tag{16}$$

where γ is the relativistic mass factor and B is the axial magnetic field. The calculation used a field amplitude factor $A = 0.012$. A is defined by

$$A = \frac{E\lambda}{8\pi \, V_n \, J_1 \, max} \tag{17}$$

where E is the peak electric field, V_n is the rest mass equivalent voltage for an electron (511 kV), and J_1 max is the maximum value of the J_1 Bessel function. The orbit center for all electrons was placed at a normalized radius of 2.

The calculation indicates that four electrons reach the end of the cavity with reduced energy, three gain energy, and one exits with the same energy as the initial beam. An average of the energy of all eight electrons at the exit of the cavity in this case indicates that the beam has transferred 10% of its initial energy to the cavity fields. This calculation could represent a solution for a single-cavity oscillator provided that the Q of the cavity and the dc beam current are high enough so that the energy removed from the beam is equal to or greater than the energy dissipated in the walls of the cavity when the assumed field amplitude is present.

The results of similar calculations, with different field amplitudes and various amounts of slip between frequency and cyclotron frequency, are shown in Figure 9.
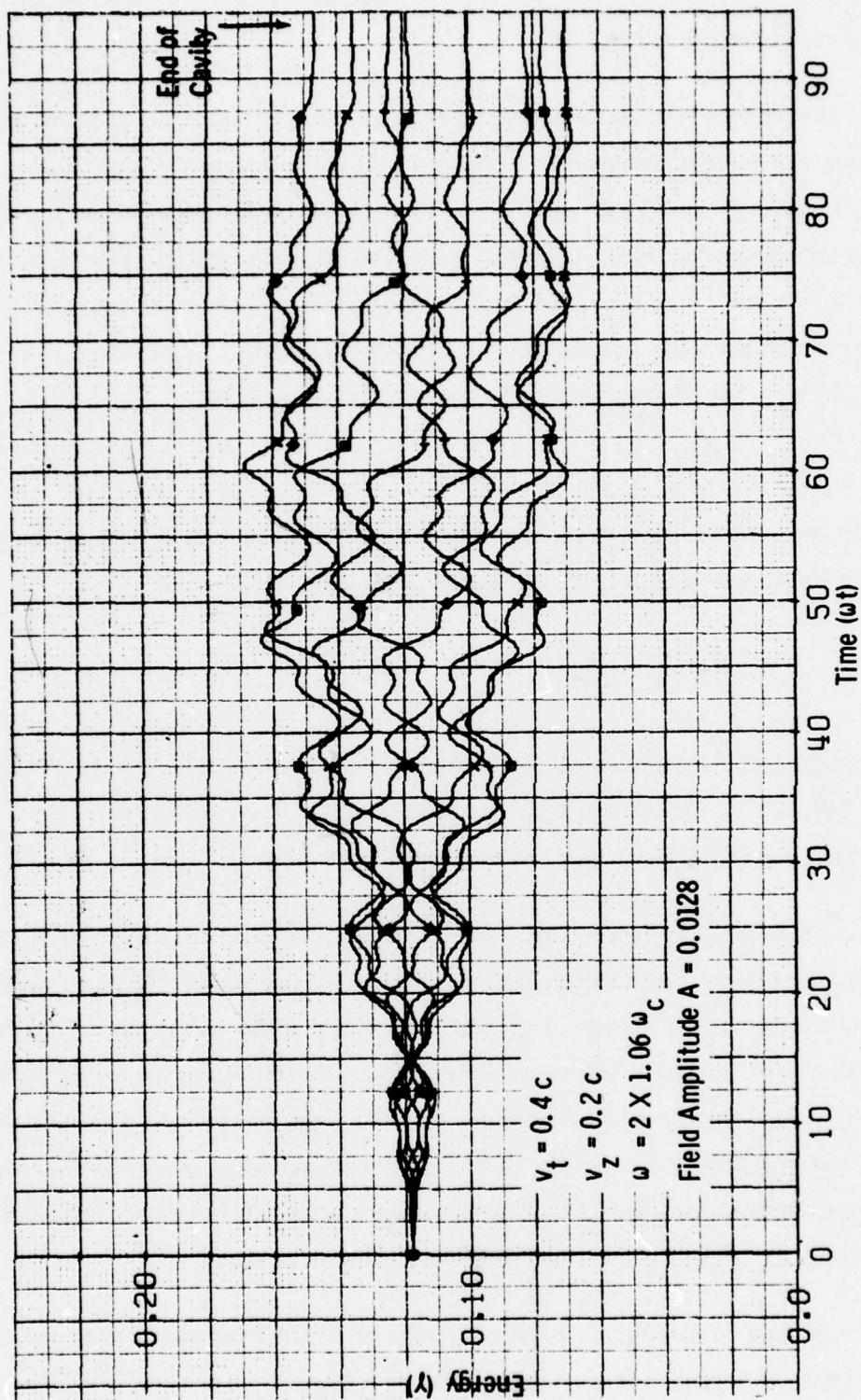
25

Figure 8. Energy vs Time for Eight Electrons Passing Through a TE$_{011}$ Cavity
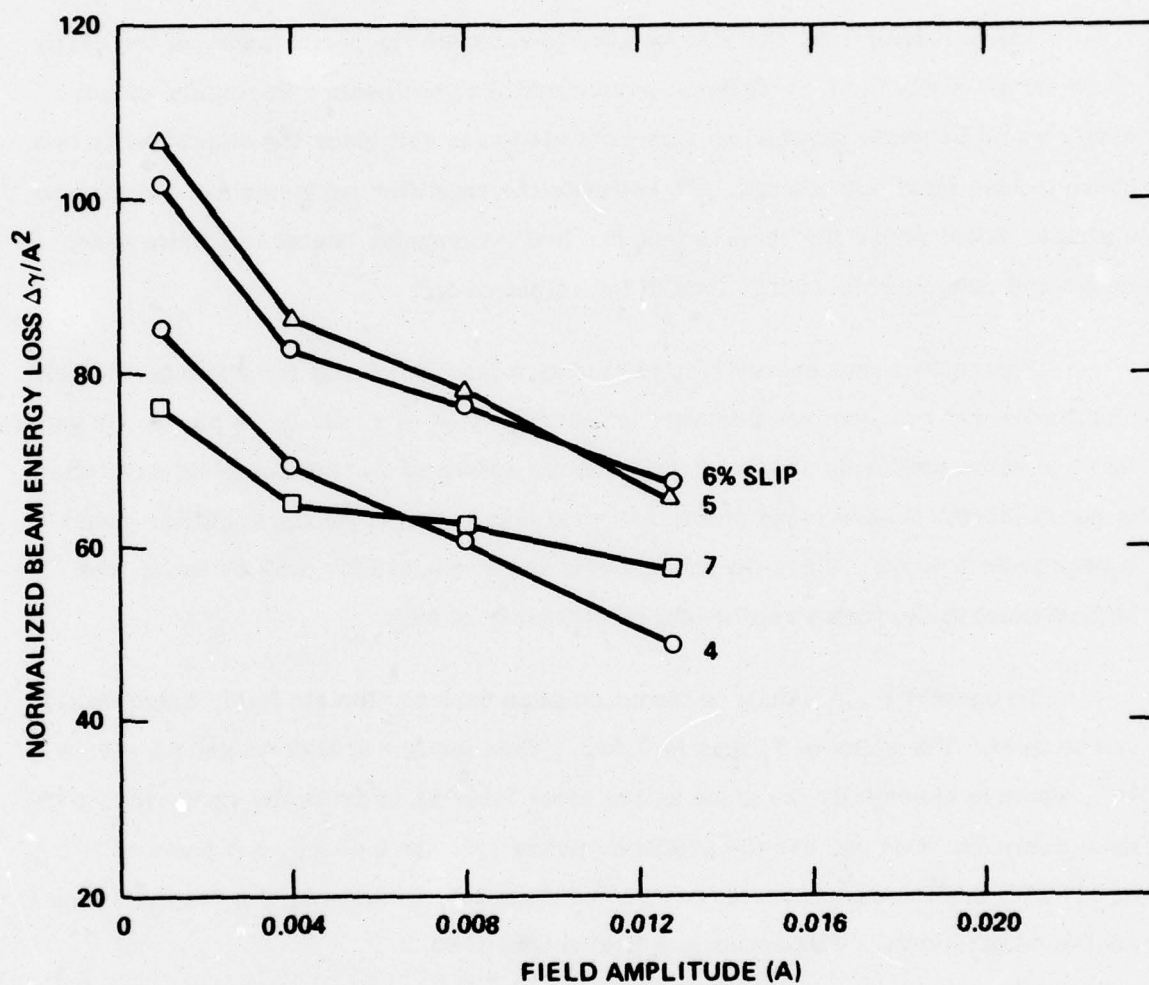
26

Figure 9. Large Signal Negative Beam Loading TE_{011} Cavity, $L = 3 \lambda$, $v_t = 0.4$ c, $v_z = 0.2$ c, Second Harmonic

The vertical axis in the figure is the beam energy loss normalized to the square of the cavity electric field amplitude. This is related to the effective negative beam loading impedance. For the parameters used in the calculation, the greatest negative loading (and therefore the most likely oscillation condition) occurs for values of slip of 5 to 6%.

These calculations can also be used to estimate the performance of the cavity as an output cavity in an amplifier. In an amplifier, the beam entering the output cavity would be phase bunched so that most electrons will enter the output cavity in a phase to lose maximum energy. To estimate the amplifier performance, we assume a simple model where the beam is bunched into rectangular bunches of finite phase length and calculate the energy loss in the output cavity.

Figure 10 shows energy loss plotted as a function of slip for a number of field amplitudes and two assumed rectangular bunch lengths of π and $3\pi/4$ phase. In general there is some indication of saturation for large values of A, but complete saturation is not reached. A good value of slip for maximum output from the amplifier would appear to be 4 or 5%. Since the initial beam has $\gamma = 0.118$ for a 60 kV beam, the highest point in the figure represents an efficiency of 39%.

To convert the A values in the calculation back to electric field, Equation (17) can be used. The value of J_1 max is 0.582. Then for A = 0.0128 we get $E\lambda = 0.96 \times 10^5$, which is essentially the same as the value determined from the earlier approximate analysis. One can use the predicted power loss for a 60 kV, 5 A beam of 39% or 117 kW, and the assumed value of $E\lambda = 0.96 \times 10^5$, to determine a required total Q for the output cavity. The result is a loaded Q of 1000.

The results of these calculations were favorable enough to allow the design to proceed based on an output cavity of length 3λ and Q 1000. For an input cavity, a length of 1.5λ was chosen so that the input cavity would be more stable than the output. An intermediate cavity was added to enhance gain. Design values of Q for the input and intermediate cavities were set at 1000 to match the output cavity Q.

28
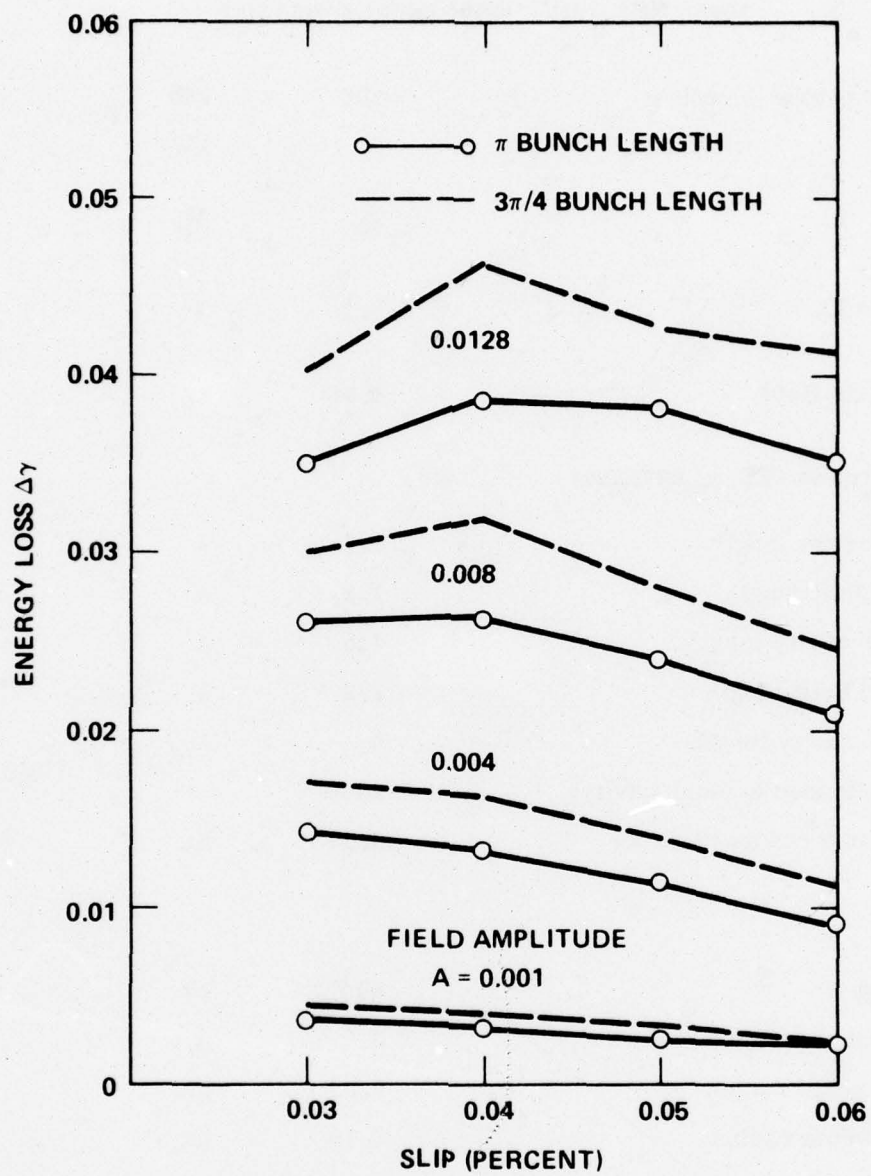
Figure 10. 3λ Output Cavity Energy Loss for Second Harmonic Interaction

A summary of the design values for the X-band amplifier is given in Table 1.

TABLE 1.

10.35 GHz AMPLIFIER DESIGN VALUES

1.	Power output — peak	100	kw
	average	5	kW
2.	Gain	30	dB
3.	Bandwidth	0.1	%
4.	Magnetic field	1.96	kg
5.	RF circuits (TE$_{011}$ cavities)		
	Input cavity length	1.5	λ
	First drift length	1.2	λ
	Center cavity length	1.5	λ
	Second drift length	1.2	λ
	Output cavity length	3	λ
	Cavity loaded Q (each cavity)	1000	
	Drift tube radius (0.51 λ)	0.58	in.
6.	Beam		
	Voltage	60	kV
	Current	5	A
	Outer beam radius	0.53	in.
	Inner beam radius	0.19	in.
	Axial velocity	0.2	c
	Transverse velocity	0.4	c
	Electron orbit radius	0.15	in.

30

B.   CALCULATION OF AMPLIFIER PERFORMANCE

The trajectory code described earlier was used to calculate overall amplifier performance in more detail. The parameter values used were the ones listed in Table 1. This calculation began with 16 electrons equally distributed around the orbit center as shown in Figure 11. The electron velocities and dc magnetic field are such that in the dc beam the 16 electrons would move along the path indicated by the circle in the figure. The orbit center for the 16 electrons is then at $X = 2.2$, where X is the normalized coordinate $X = 2\pi x/\lambda$. In the real device, both the beam and the microwave fields have complete angular symmetry about the $X = 0$, $Y = 0$ axis.

To proceed with the calculation, the electrons as shown in Figure 11 are injected into the input cavity with the appropriate components of dc velocity. During the transit of the electrons through the input cavity, some electrons gain energy and others lose energy depending on their angular position with respect to the cavity fields. The result is shown in Figure 12. The most obvious change is the overall rotation of the pattern, but some angular bunching and change in orbit radius can be detected. On the average, all electrons have lost 0.04% of their initial energy, indicating that the input cavity has positive beam loading. In this case the normalized electric field amplitude used in the calculation for the input cavity was $A = 0.0015$. With an input cavity Q of 1000 this would be achieved with an input power of 500 W. The magnetic field in the calculation was set for a slip of 4% from the second harmonic cyclotron resonance.

Figure 13 shows the electron positions after the first drift region just prior to entering the intermediate cavity. Further rotation of the pattern and some additional angular bunching have occurred at this point.

Next, the electrons are passed through the intermediate cavity. In this case, an iterative procedure is used with various phases of the cavity field to determine the phase which results in maximum energy loss by the electrons. That phase corresponds to the situation where the cavity is tuned to the same frequency as the input
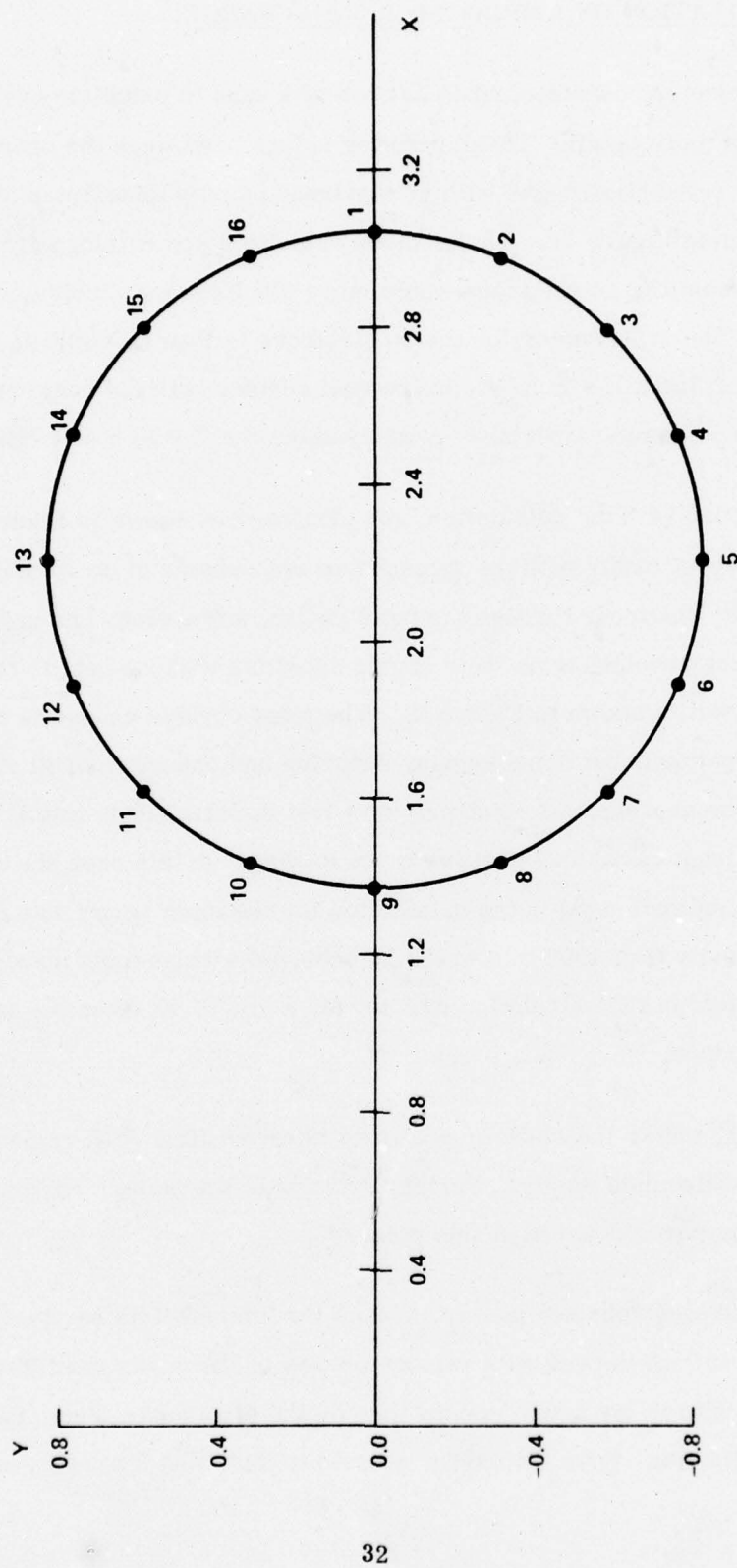
31

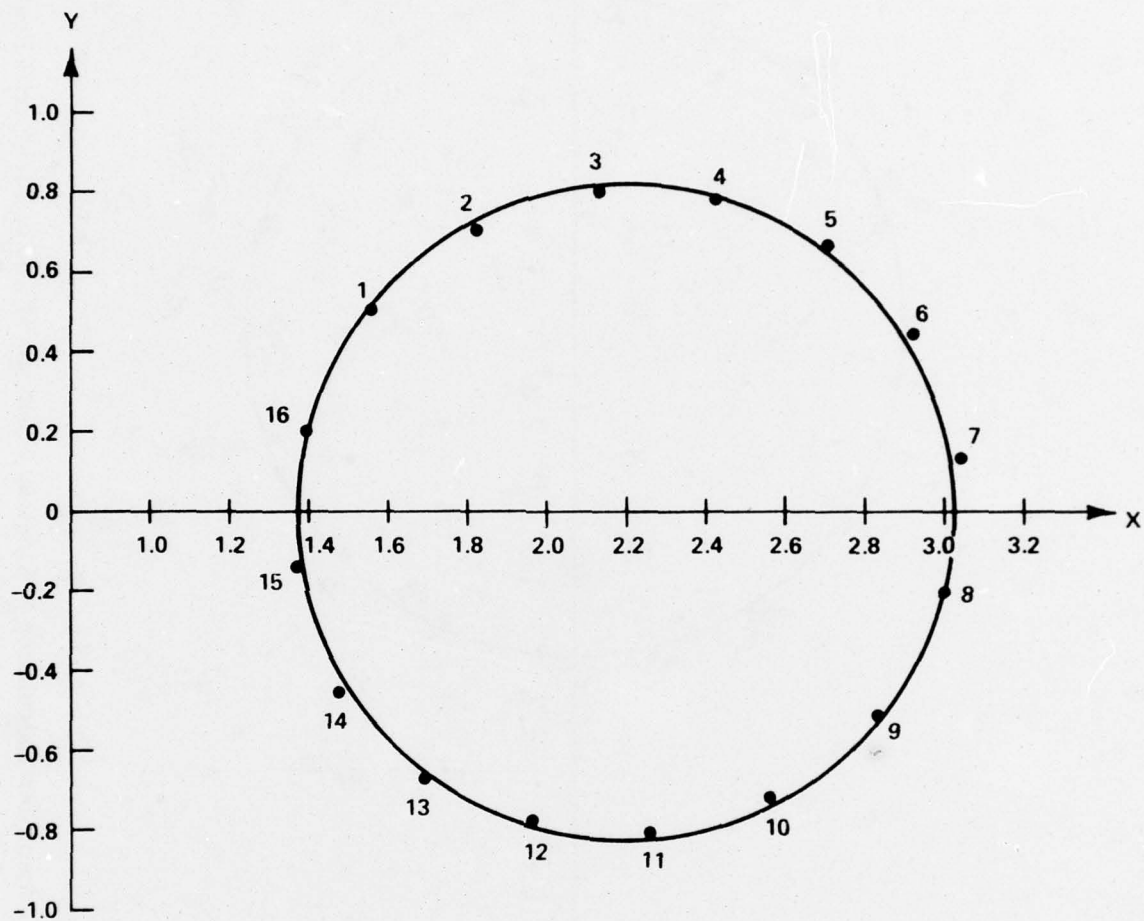Figure 11. Amplifier Calculation – Electron Positions at Beginning of Input Cavity

32

Figure 12. Amplifier Calculation – Electron Positions at End
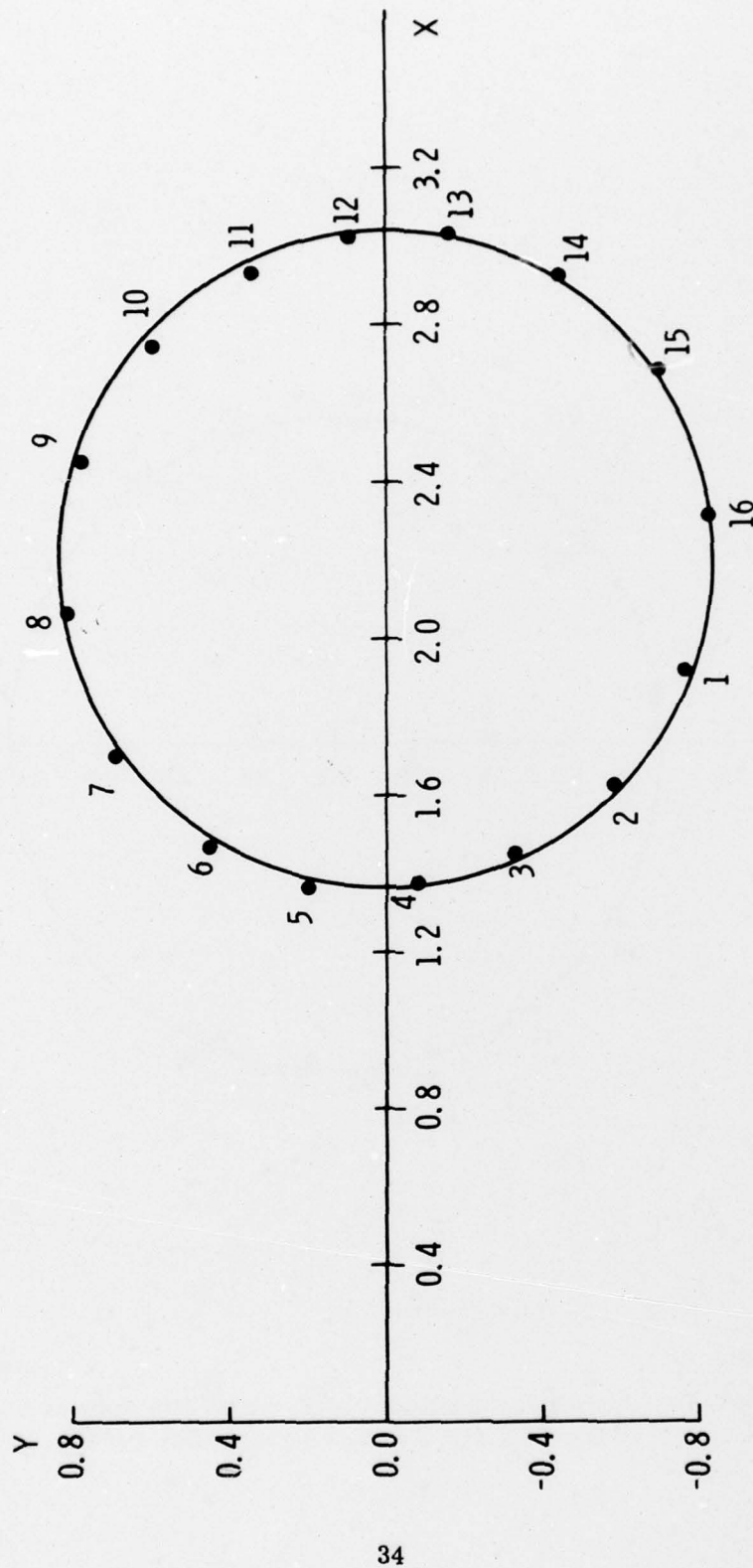of Input Cavity; Average Energy Gain 0.04%

33

Figure 13. Amplifier Calculation – Electron Positions at End of First Drift Region

34

cavity and presents a resistive load to the beam. The result with the field having that phase is shown in Figure 14. The average energy loss for all electrons is now 1.4%, or about 4 kW for a 5 A beam. It is also clear from the figure that additional energy modulation and angular bunching have taken place during transit through the cavity.

Figure 15 shows the electron positions at the end of the second drift region. Increased angular bunching is evident. It should be noted that the presence of two regions of bunched electrons is characteristic of the second harmonic cyclotron interaction. The fact that the two bunches are not totally symmetric with each other is because the cavity fields are not totally symmetric from one side of the orbit to the other.

Figure 16 shows the electron positions at the end of the output cavity. The average energy loss of all electrons is 37.5%, or 112 kW. This number includes the 4 kW removed by the intermediate cavity. Therefore the total output power would be 108 kW or 36%, less any output cavity losses. It is clear from the figure that most of the electrons have moved to smaller orbit radii in losing energy. Two electrons have gained energy and lie outside the normal dc orbit circle. This is expected since the bunching was never completely accomplished.

A power output of 100 kW together with the 500 W input power represents a gain of 23 dB. This was somewhat below the design goal of 30 dB. However, it is expected from the calculations of Kovalev[14] and Kosolov[15] that space-charge effects will increase the gain of an amplifier compared to the ballistic value. Therefore, the proposed design values were considered reasonable for a first experiment.

C.   ELECTRON GUN DESIGN

The favored approach for producing an electron beam with the required high transverse energy and small velocity spread was the magnetron gun configuration described by Gol'denberg[16]. To determine the detailed shape of the electrodes, computer simulation was used employing a Varian proprietary gun analysis code. This code has been used for many years to design guns for high power microwave tubes.
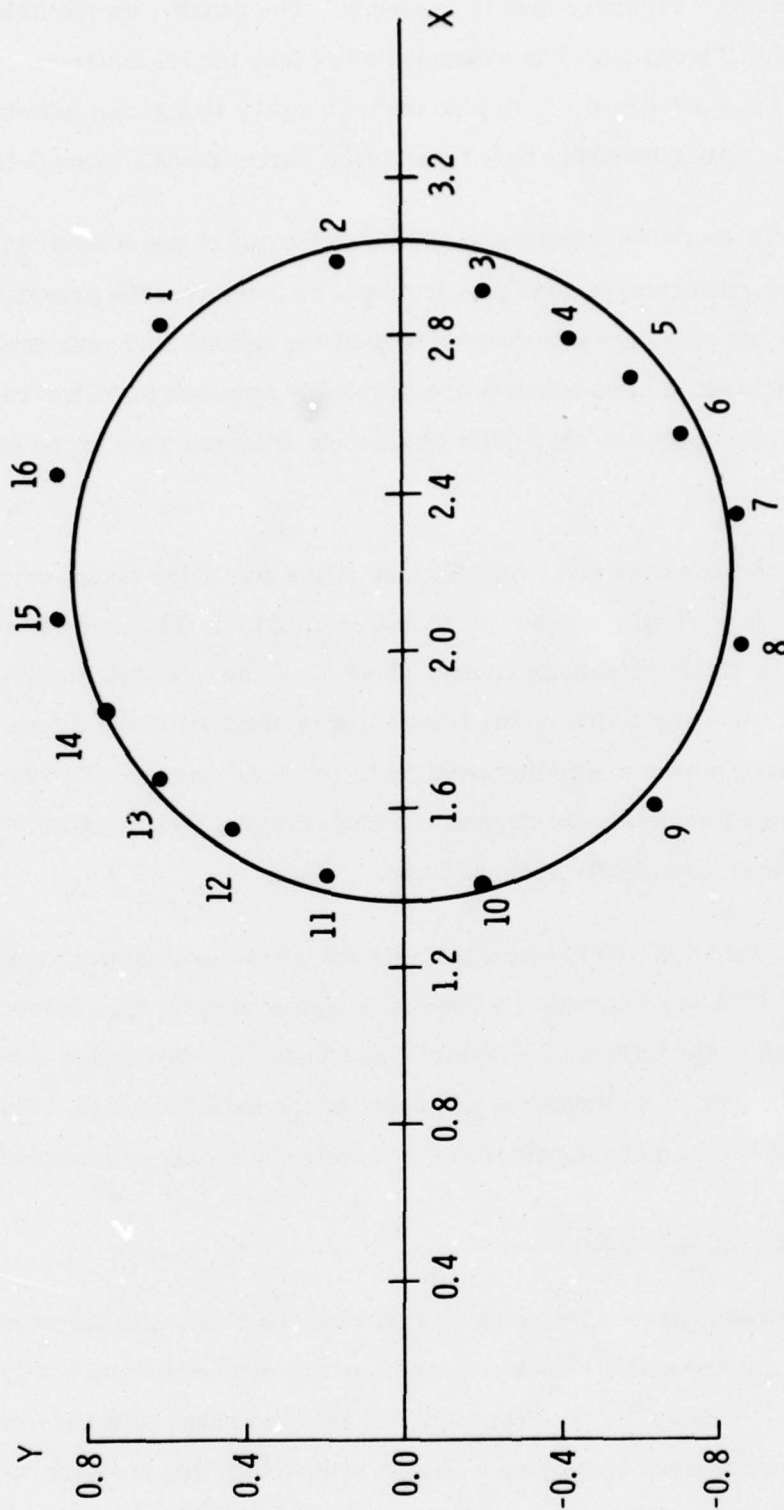
Figure 14. Amplifier Calculation – Electron Positions at End of Intermediate Cavity
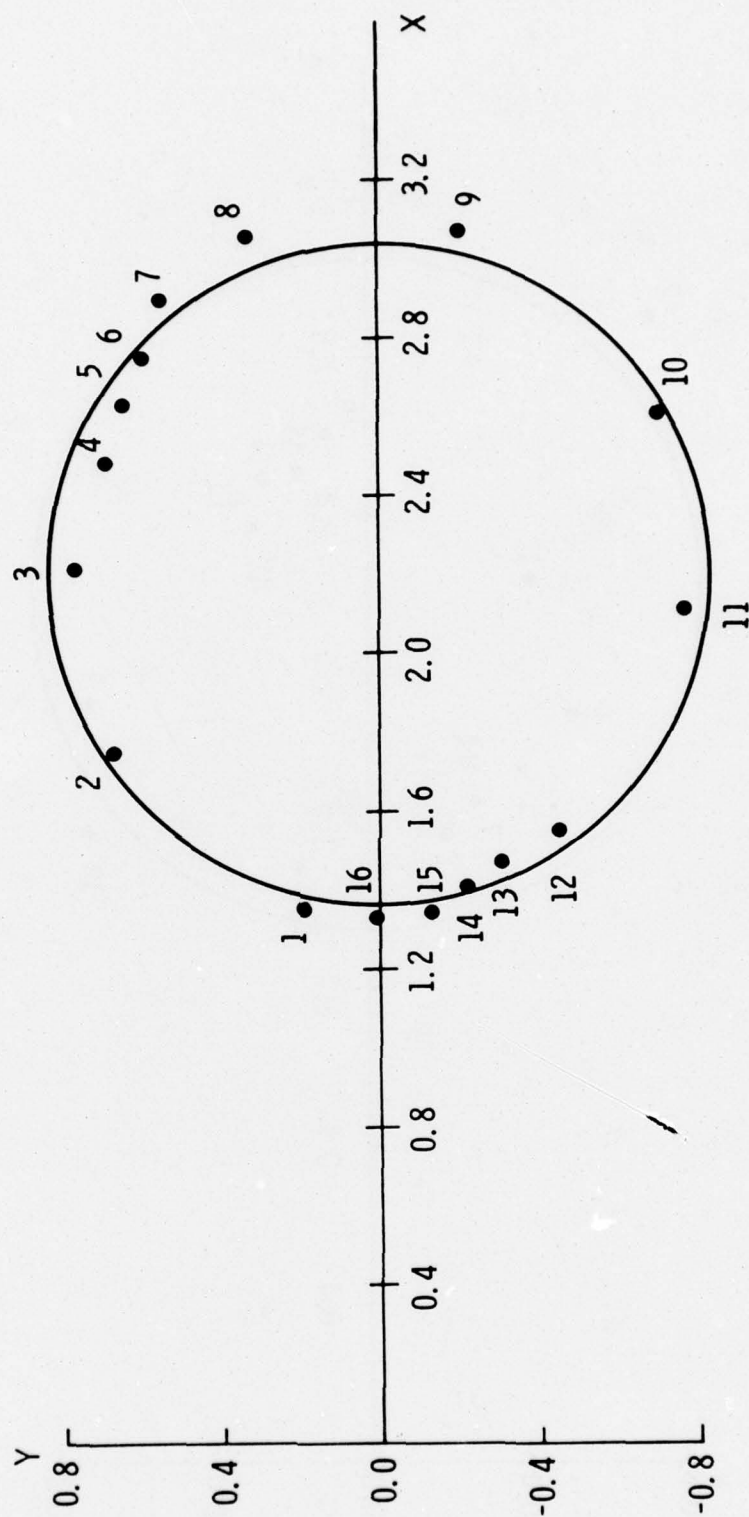Average Enérgy Loss 1.4%

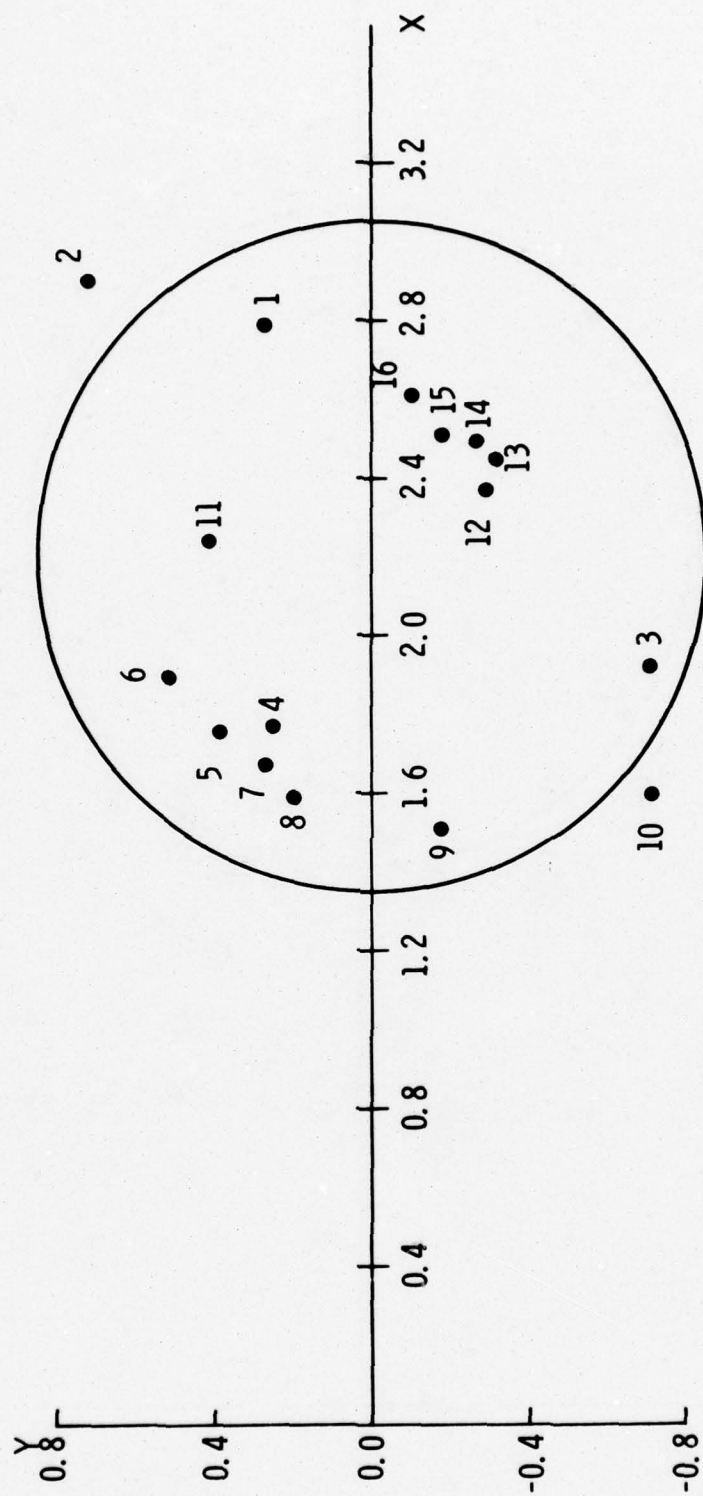Figure 15. Amplifier Calculation — Electron Positions at End of Second Drift Region

37

Figure 16. Amplifier Calculation – Electron Positions at End of Output Cavity
Average Energy Loss 37.5%

38

The code includes space charge and relativistic effects and can operate with a two-dimensional, spatially varying, dc magnetic field.

A magnetic field compression ratio of 4 between gun field and interaction field was chosen as being a reasonably conservative value based on the Russian publications. Then the design field at the cathode becomes 485 g. The resulting radial compression was a factor of 2, and the desired radial position of the orbit centers in the interaction region then determines the average cathode radius of 0.66 inch. The cathode length was taken to be 0.35 inch, which results in an operating current density of 0.5 A/cm^2. A low cathode current density was desirable to minimize problems in later scaling the device to 94 GHz. With the value chosen, only a modest redesign of the gun will be needed, and there was some concern that making the cathode longer might make the design of the initial device overly difficult.

The optimization of the performance of the gun required several empirical iterations on electrode shapes and on the magnetic field profile. A simulation of electron motion for the final design is shown in Figure 17. The beam voltage and current for that case were 60.3 kV and 5 A. The cathode model used temperature-limited emission. The intermediate electrode (gun anode) was operated at 31 kV above cathode potential. The calculated axial velocity in the simulation, after magnetic compression, had an average value of 0.208 c compared to a design goal of 0.2 c. The peak calculated spread in axial velocity was ± 5%.

The gun was designed to use standard techniques in construction. The only unusual feature of the construction was that the conical front focus electrode was designed with oil-cooling channels. Since this electrode must be supported through the hollow cathode, there was concern that heat radiation from the heater and cathode would cause the front focus electrode to run hot enough to emit electrons. Even though the electron emission density might be quite small, the area of the electrode is an order of magnitude greater than the cathode area. The gun anode was also designed with oil-cooling channels in case beam interception might be encountered. Since the anode operates about 30 kV off ground potential, water cooling was not ideal.
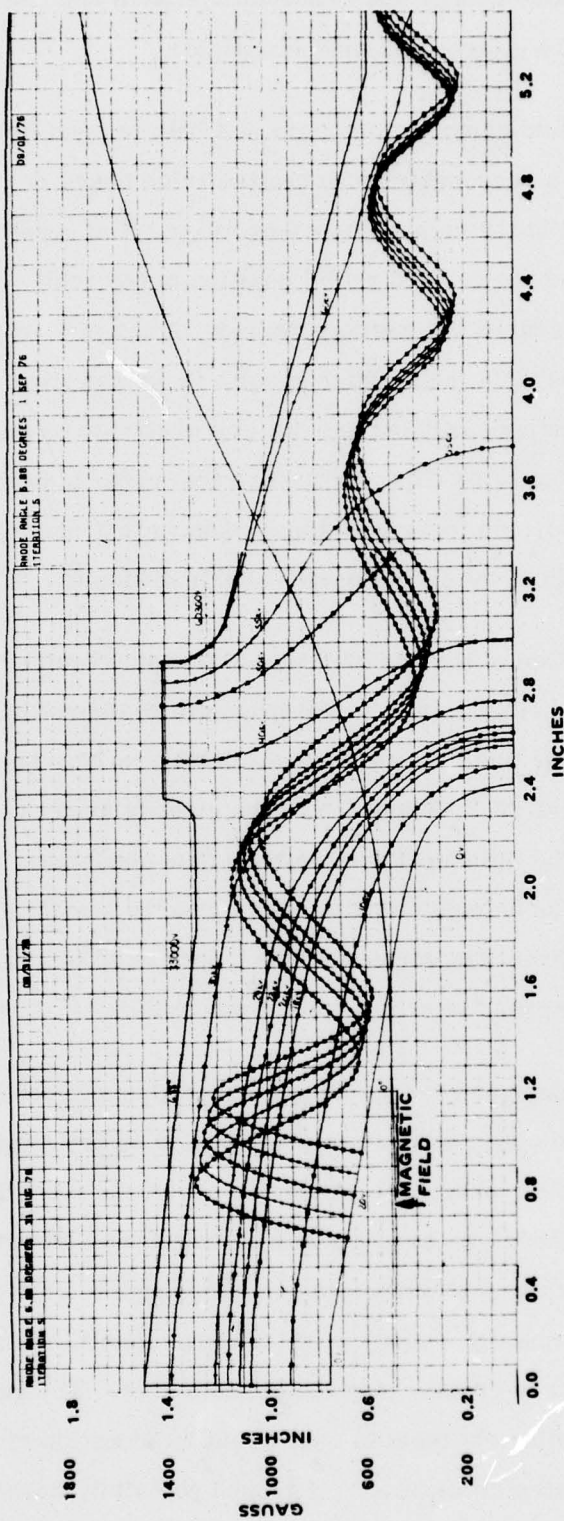
39

Figure 17. Gyrotron Gun Simulation

It was intended that a small, submersible oil pump be used to supply about 1 gpm oil flow for both the focus electrode and anode cooling.

The cathode was designed as a conventional impregnated cathode, except that some care was taken to obtain as smooth a surface on the cathode as possible. The heater was potted in alumina as an integral part of the cathode assembly.

D.   MAGNET DESIGN

Calculations were performed using the trajectory code to determine the effect of a spatial variation in the dc magnetic field on amplifier performance. It was found that a variation of 5% over the length of the output cavity had very little effect. A reduction in magnetic field toward the output end of the tube actually improves efficiency by a few percent, in some cases, as one might expect from the increase in angular velocity which occurs as the electrons lose energy. In any case it was concluded that super uniformity in the magnetic field was not needed. Therefore a fairly conventional solenoid design was used to supply the main magnetic field.

The solenoid had a 6-inch diameter inner bore and an axial length of 16 inches. The windings were divided into four equal sections which allowed control over the axial field profile. The magnet was capable of continuous operation at 2500 g. Pole-pieces were used which had a 3.25-inch inner diameter at the collector end and a 4-inch inner diameter at the gun end. The large-diameter holes in the polepieces were used in order to minimize possible problems in later scaling to 94 GHz.

Gun simulations indicated that the most critical part of the magnetic design was the shape of the field profile in the gun region. A change in the field shape involving a slight variation near the cathode was shown to produce large changes in beam quality. To give control of the gun field in practice, an additional coil was used surrounding the gun region. This coil has an inner diameter of 5.5 inches and an axial length of 2 inches. It was capable of producing 500 g at the cathode.

41

To insure that the gun design would be compatible with the achievable magnetic field, the solenoid and gun coil were set up in the laboratory and the axial magnetic field profile was measured. The measured field was then used in the gun simulation to calculate beam performance.

E.   TUBE BODY DESIGN

Figure 18 shows a cross section of the X-band three-cavity gyroklystron amplifier and its relationship to the solenoid and gun coil. The body was designed with a number of subsections welded together so that later modification of one or more sections could be easily accomplished. The gun and gun coil were designed to be operated in oil with the axis of the tube vertical and the oil level just below the end of the main solenoid.

Most of the body parts are copper. Stainless steel rings are used at the weld joints. The input cavity is loaded to a Q of 1000 by coupling it to three waveguides. Two of these guides are terminated in later loads as an integral part of the tube envelope. The third guide is the input guide. The center cavity is loaded to a Q of 1000 by a coating of Kanthal on its inner surface. The output cavity is loaded to a Q of 1000 by the large coupling port leading through the collector to the output window.

The output guide is 2 inches in diameter. This allows propagation of the TE_{01} cylindrical mode at 10.35 GHz but prevents propagation of the TE_{02} mode at that frequency. There is an axial break in the wall of the output guide just outside the output cavity and prior to the collector region. This break has little effect on the TE_{01} propagation and allows collector current to be measured directly. The beam collector is basically a section of the output waveguide that is thoroughly water cooled. The collector region is capable of 100 kW power dissipation provided the beam is distributed over most of the cooled area.

The tube was pumped and processed in a conventional manner. A 2 ℓ/sec VacIon® Pump was left attached to the tube so that pressure could be monitored during test.
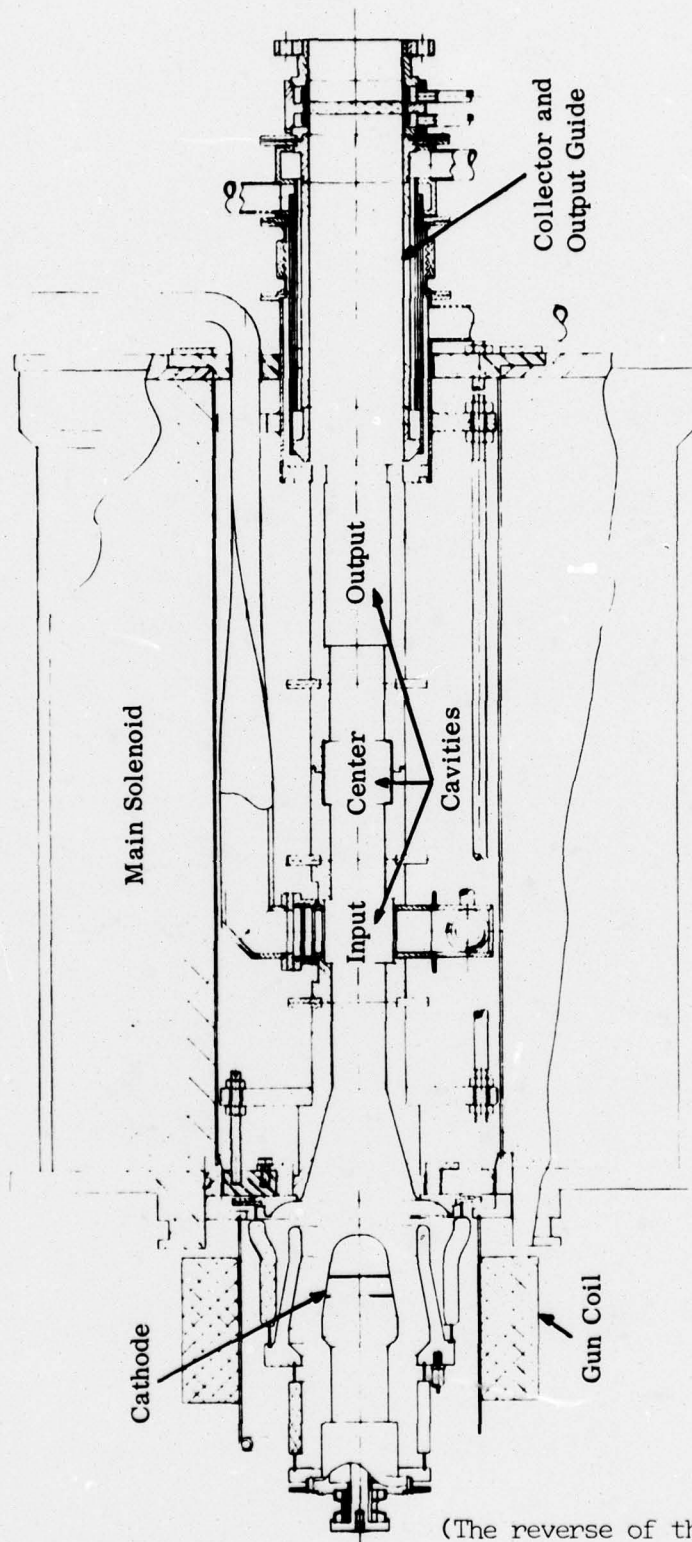
Figure 18. Layout of 10.35 GHz Gyroklystron

(The reverse of this page is blank)

43

V. INITIAL TEST RESULTS

A. DESCRIPTION OF TEST FACILITY

The X-band gyroklystron amplifier was installed in a test facility capable of supplying 0 to 60 kV with pulse currents exceeding 10 A. A block diagram of the connections to the gyrotron and the instrumentation available is shown in Figure 19. The pulsed source is a dc power supply with a series vacuum switch tube. The voltage applied to the gun anode is obtained from an RC divider between cathode and ground. In addition to the various current measurements indicated in the figure, there is a divider available which can be used to measure pulsed cathode or gun anode voltage.

The power supplies furnishing beam voltage, heater voltage, and current to the four main magnet sections are all unregulated supplies. Even so, the operation of the gyrotron is sufficiently stable to allow reasonable measurements to be made. The gun coil current was found to be reasonably critical. A regulated supply is used to control that current.

The output waveguide (2-inch diameter pipe) is terminated by a ceramic cone with water behind the cone. The temperature rise in the water is used to determine average power output. The pulse shape and frequency of output power are determined using a power sampler. The sampler consists of an X-band rectangular guide coupled through a small hole in the wall of the output pipe. The rectangular guide is oriented so that it couples to any mode in the output guide that has an axial component of H. Thus, all TE modes in the pipe are sampled.

A rectangular-to-circular guide transition was used with a signal generator to calibrate the signal sampler. For the TE_{01} cylindrical mode in the pipe at 10.35 GHz, the coupling ratio to the sampler is -37 dB.

Microwave power was supplied to the input by a sweep generator followed by a 10 W TWT amplifier. During the initial testing a higher power driver was not available.

45
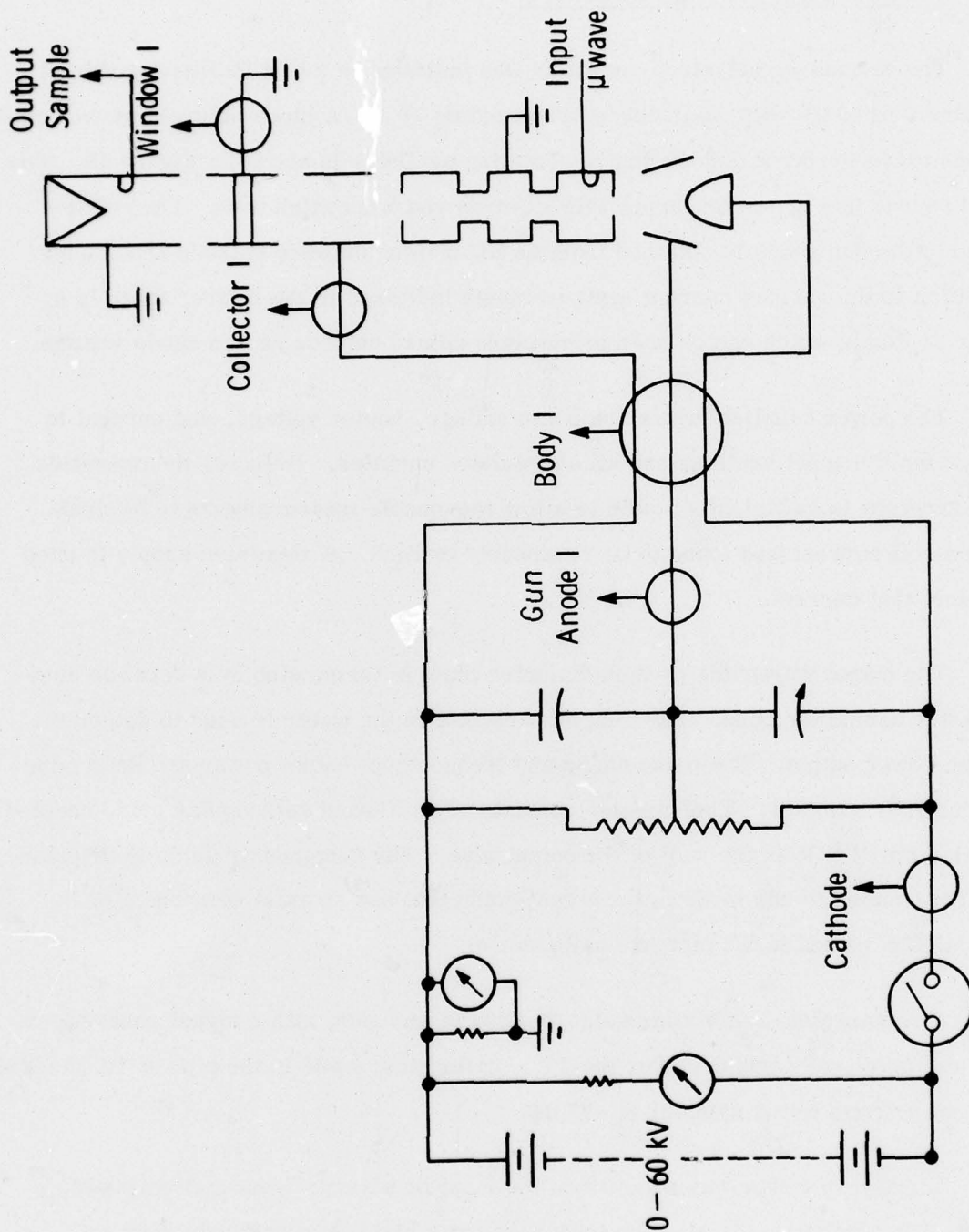
Figure 19. Test Connections for Gyrotron

46

A system to monitor for C-band oscillation output consisted of an open-end C-band waveguide located in the oil tank near the gun insulators. This led to a crystal detector through appropriate filters with a wavemeter to measure frequency.

A directional coupler was included in the input line to monitor any reflected power or oscillation power coming from the input cavity. This system is limited to X-band or above, since there is a fairly long section of X-band rectangular guide leading to the input cavity.

B.   AMPLIFIER RESULTS AND DIAGNOSIS OF OSCILLATIONS

During initial operation, we observed a microwave gain of 9 to 10 dB under small signal conditions where power output is about 100 w peak. This operation was achieved at a reduced beam voltage of 40 kV. Attempts to increase gain have invariably led to the onset of C-band oscillations. Increases in beam voltage result in an increased tendency toward oscillation. A summary of initial test results is shown in Table 2.

TABLE 2.

SUMMARY OF INITIAL TEST RESULTS

Parameter	Design Value	Test Value
Beam voltage	60 kV	40 kV
Gun anode voltage	31 kV (52%)	24 kV (60%)
Beam current	5 A	4.5 A
Main magnet field	1960 g	1960 g ± 5%
Gun magnet	485 g	450 g ± 10%
Microwave gain	23 - 26 dB	9 - 10 dB
Peak body current	0	80 ma
Peak gun anode current	0	10 ma

47

In typical operation, there are three parameters which have a significant effect on gain. These are beam current, gun coil current, and main magnet current. Increases in gun coil current reduce the gain, and decreases in gun coil current increase gain to a point where oscillations appear. This behavior is not unexpected, since decreases in gun coil current should increase the transverse energy of the beam, which should enhance either amplification or oscillation. Increases in beam current also enhance either oscillation or gain.

With respect to the main magnet field, under maximum gain conditions there is an optimum value for the magnet current in each of the four sections of the magnet. However, if any magnet section is set to a slightly higher current, the C-band oscillation appears and amplifier gain decreases abruptly. If the current in any of the four sections is decreased, the amplifier gain smoothly decreases. Typically, a decrease of 0.25 A out of 9 A in any magnet section results in a loss of gain of 3 dB. Assuming the same variation would apply on the high current side if oscillation were not present, the gain sensitivity to one magnet section would be ± 2.8% for 3 dB variation. If all four magnet sections were varied together, a sensitivity of ± 0.7% would be expected for 3 dB gain variation. The gun coil sensitivity is +1.5% for a 3 dB gain variation.

Considerable overlapping or interdependence was observed among the four sections of the main magnet. This was expected since there was no magnetic isolation between sections. Typically a change of 0.5 A in one section can be compensated for by a change in other sections. Hence there is not a completely unique profile which gives optimum gain.

The oscillations which interfere with amplifier operation appear initially at a frequency of 5.430 GHz. By varying the currents in the main magnet sections, it is possible to tune the frequency of oscillation and to introduce what appear to be other modes of oscillation. For example, variation in the main magnet section closest to the gun results in two modes of oscillation, one of which tunes from 5.424 to 5.433 GHz and the other from 5.425 to 5.471 GHz.

48

The main magnet section near the gun has the most effect on the power and frequency of the C-band oscillations. The section near the collector has very little effect. This behavior suggests that the input end of the tube is the location to look for resonances which might support the oscillations.

The drift tubes have an inner diameter of 1.155 inches. The lowest mode which can propagate in the drift tube is the TE_{11} which has a cutoff frequency of 6.05 GHz. Therefore, the oscillation frequencies are nonpropagating in the drift tubes, but are not far from cutoff. A cold test model which has dimensions similar to the actual tube showed that the input and center cavities have TE_{111} resonances at 5.405 and 5.399 GHz, respectively, when measured as separate cavities. However, when the two cavities are connected by the drift tube configuration used in the tube, the two resonances couple together by virtue of the limited attenuation of the cutoff drift tube. The resonant frequencies of the coupled system are 5.419 and 5.385. The cold test measurements indicate that energy is shared rather equally between both cavities at both frequencies.

It appears likely that the measured oscillation frequencies in the tube are related to these resonances. The difference between the oscillation frequencies and the cold test frequencies could be explained by fairly small dimensional differences.

From the values of main magnet field for which these oscillations occur, it is clear that they involve the fundamental cyclotron resonance interaction. When the second harmonic amplifier is optimized for operation at 10.35 GHz, the beam will be near optimum for fundamental interaction at 5.18 GHz.

When these C-band oscillations occur, large amounts of power are radiated from the gun end of the tube through the gun insulators into the oil tank. There is also considerable microwave radiation through the insulators at the output end of the tube. Whereas these insulators do not radiate when the TE_{01} cylindrical wave propagates in the output guide, one would expect them to radiate any TE modes that have axial wall currents. The large amount of radiation led to speculation that an external

49

feedback path might be enhancing the oscillations. Efforts to improve stability with external absorbers were not successful, however.

With the main magnet set at lower field, another type of oscillation could be observed coming out the input waveguide at a frequency of 8.512 GHz. This frequency correlates with the TE_{211} resonance in the input cavity which had a measured value of 8.491 GHz in cold test. This resonance does not produce much power in the output guide. The magnetic field values for this oscillation indicate that it is occurring at the second harmonic of the cyclotron frequency.

Another oscillation was observed with a different reduced main magnet field at a frequency of 8.330 GHz. This correlates with the TE_{211} resonance in the output cavity which was measured at 8.320 GHz during cold test. Furthermore, this oscillation is particularly sensitive to currents in magnet sections near the collector end of the tube. Considerable power was observed in the output guide with this oscillation, and microwave radiation through the insulators at the collector end of the tube was quite high. With operation at a duty factor of 10^{-3} the output power was measured by the water load and found to be 19.5 W average. This represents a peak output power of 19.5 kW. Beam parameters were 40 kV, 5 a peak for an efficiency of 9.8%. A correction for power radiated through the insulators would result in a higher output power number. The magnetic field value for this oscillation again indicates operation on the second harmonic of the cyclotron frequency. In this case very little power comes out the gun end of the tube or the input guide.

The presence of oscillations at many frequencies, although a detriment to amplifier performance, is encouraging in the sense that it indicates that the beam transverse velocity must be large and that the spread in velocity must be small. It would be most useful to be able to evaluate the beam velocity distribution more quantitatively; then, direct comparison of calculated and measured performance could be made. Methods of evaluating the beam need to be studied.

On the basis of the initial measurements it is concluded that the beam performance is close to the desired performance. The gross feasibility of a gyroklystron

50

amplifier has been demonstrated. Modifications to the existing amplifier are needed to improve stability. Selective loading, in which loss is introduced into axial breaks in the microwave circuits, should accomplish the desired loading.

(The reverse of this page is blank)

VI. BANDWIDTH OF GYROKLYSTRON AMPLIFIERS

The bandwidth of a gyroklystron with resonant cavities is limited primarily by the properties of the output cavity. To investigate the bandwidth, we begin with the basic definition of tube efficiency

$$\eta = \frac{P}{I_b V_b} \tag{18}$$

where P is the power output, I_b is the dc beam current, V_b is the dc beam voltage, and η is efficiency. For high efficiency operation we must have

$$\Delta V \approx V_b \tag{19}$$

where ΔV is the effective circuit voltage or the voltage equivalent of energy lost by an electron traveling through the output circuit.

We can combine Equations 18 and 19 into the form

$$\frac{V_b}{I_b} = \eta \frac{(\Delta V)^2}{P} \tag{20}$$

We define a parameter R/Q by the equation

$$\frac{R}{Q} = \frac{(E\lambda)^2}{2\,QP} \tag{21}$$

where E is the peak transverse electric field in the cavity, and Q is the usual quality factor defined by

$$Q = \frac{\omega U}{P} \tag{22}$$

where U is stored energy. If the P in Equation 22 includes only wall losses, then the corresponding Q is the intrinsic Q. In this discussion we will consider heavily loaded

53

cavities where the intrinsic Q is very high; then the Q in Equation 22 is the total Q and P the total output power.

The parameter R/Q can be evaluated by combining Equations 21 and 22 and calculating the stored energy in terms of the electric field amplitude. The result is

$$\frac{R}{Q} = \frac{8 \sqrt{\mu_o/\epsilon_o} \; J_o'^2 (p_{01}'')}{\pi^2 J_o^2 (p_{om}')} \; \frac{\frac{a}{L}}{\left[\left(\frac{p_{om}'}{\pi}\right)^2 + \left(\frac{a}{L}\right)^2\right]^{3/2}} \tag{22}$$

where a is the cavity radius, $J_n (kr)$ is the Bessel function of nth order and first kind, primes indicate its differentiation with respect to kr, and $p_{n,m}''$, for example, is the mth value of kr which makes $J_n'' (kr) = 0$. Curves of R/Q for TE_{0m1} cavities are given in Figure 20. A more detailed discussion of the above parameters can be found in reference[17].

The effective circuit voltage for a gyrotron cavity for the fundamental cyclotron interaction is given by Equation 14 (repeated here from Section IV).

$$\Delta V = \frac{1}{\pi} \; E\lambda \; \frac{L}{\lambda} \; \frac{v_t}{v_z}$$

where L is the cavity axial length, v_t is the transverse component of electron velocity, and v_z is the axial component. For cyclotron harmonic interactions, we can write (Equation 15 from Section IV)

$$\Delta V = \frac{1}{\pi} \; E\lambda \; \frac{L}{\lambda} \; \frac{v_t}{v_z} \; F_n$$

where F_n is the factor by which the effective voltage in the cavity is reduced by operation at the nth harmonic of the cyclotron frequency.

Combining Equations 20, 21 and 15, we get

$$\frac{1}{Q} = \frac{2\eta}{\pi^2} \left(\frac{L}{\lambda}\right)^2 \left(\frac{v_t}{v_z}\right)^2 \frac{R}{Q} \frac{I_o}{V_o} F_n^2 \tag{24}$$
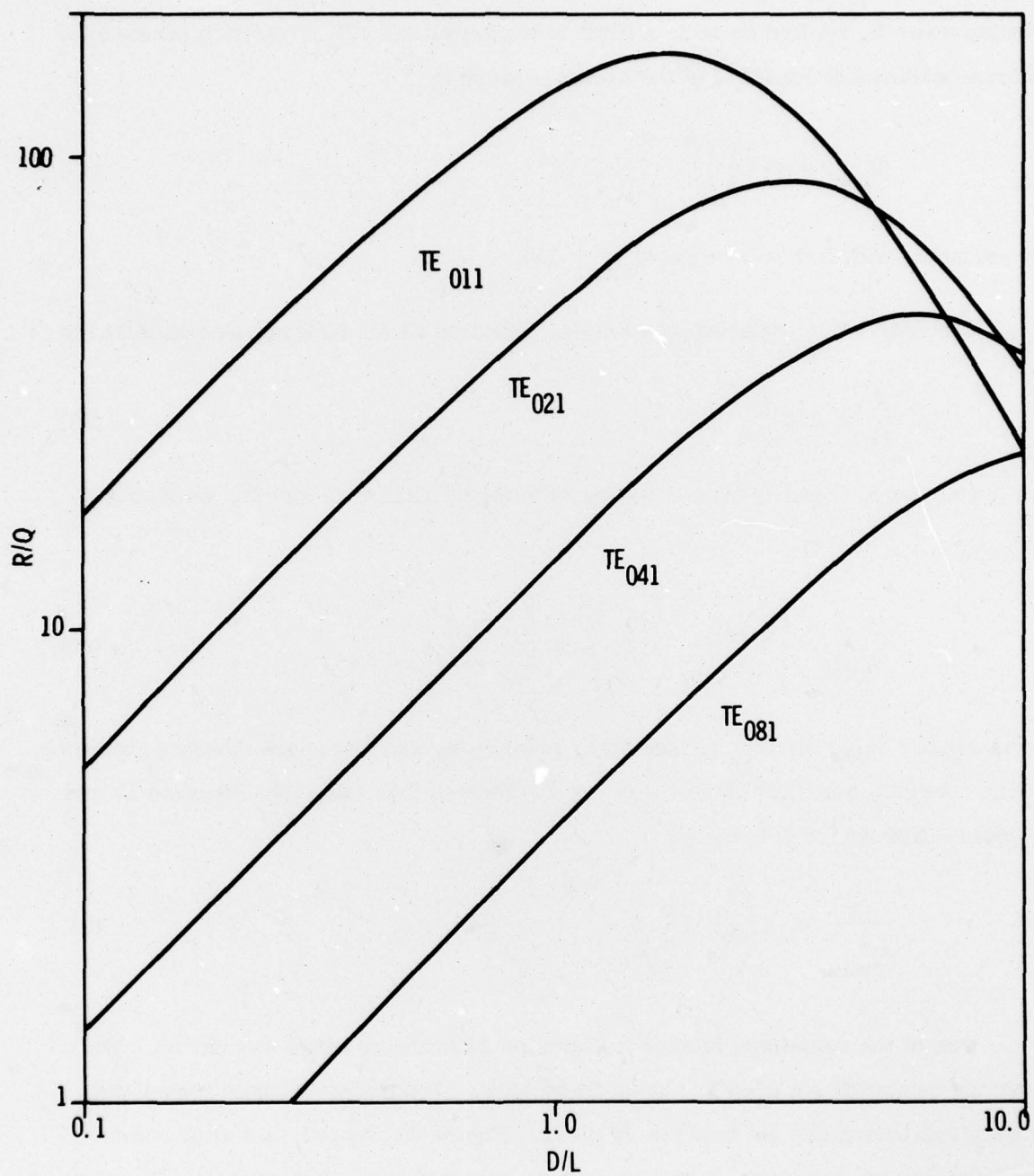
54

Figure 20. $R/Q = (E_\phi \lambda)^2 / 2 \omega U$ vs D/L for $TE_{0,m,1}$ Cavities

In this equation, $1/Q$ is essentially the output circuit bandwidth. To maximize bandwidth, it is desirable to make all the terms on the right hand side as large as possible. If we increase L, we find there is a limit to bandwidth for TE_{011} cavities because the minimum achievable loaded Q of the cavity is given by[18]

$$Q_{min} = 4\pi \left(\frac{L}{\lambda}\right)^2 \quad . \tag{25}$$

For example, with $L/\lambda = 3$ we get $Q_{min} = 113$.

For long TE_{011} cylindrical cavities, Equation 23 for R/Q can be simplified to

$$\frac{R}{Q} \approx 216 \frac{\lambda}{L} \tag{26}$$

If we eliminate R/Q and L from Equation 24 using Equations 25 and 26, we then get, for Q_{min}:

$$\frac{1}{Q_{min}} = \left[\frac{216}{\pi^2 \sqrt{\pi}} \left(\frac{v_t}{v_z}\right)^2 \eta \frac{I_o}{V_o} F_n^2 \right]^{2/3} \tag{27}$$

The maximum value of v_t/v_z is limited by velocity spread and space charge depression effects. A practical limitation is $v_t/v_z \approx 2$. Putting this value into Equation 27 and taking an efficiency of 0.3, we get

$$\frac{1}{Q_{min}^2} \approx 6 \left(\frac{I_o}{V_o} F_n^2\right)^{2/3} \tag{28}$$

One of the remaining factors in Equation 28 is the dc beam impedance. To maximize bandwidth we need low beam impedance. The limits on beam impedance for gyrotron beams are not completely clear. Figure 21 shows a plot of dc beam impedance versus frequency for the gyrotrons reported in the literature[10, 11]. The points appear to fit a simple wavelength scaling law which is reasonable but perhaps not totally justified. For a frequency of 94 GHz, a beam impedance of 2×10^4 is
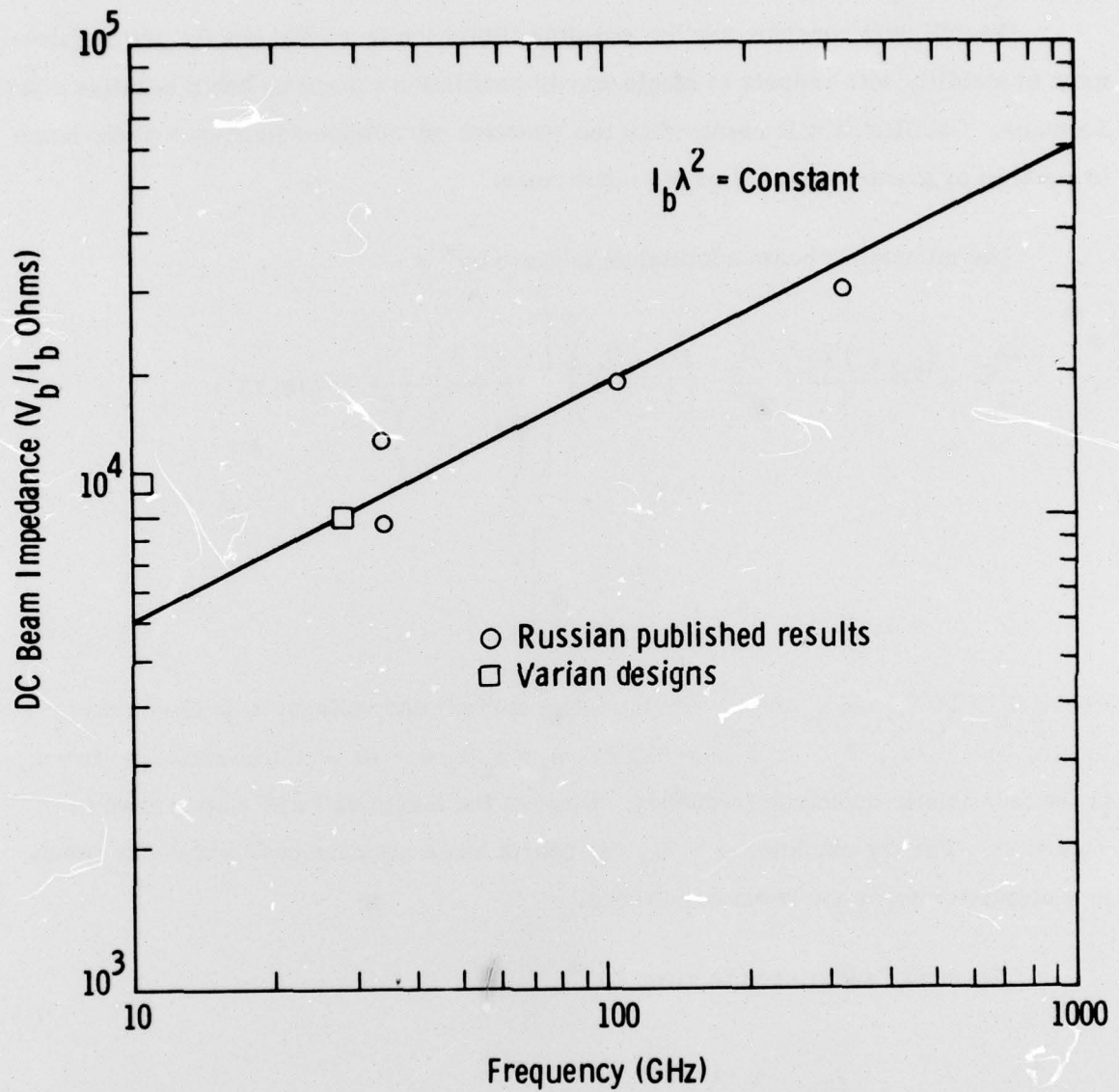
56

Figure 21. Gyrotron Beam Impedance

57

clearly reasonable. Then, for the fundamental interaction with $F_n = 1$, a bandwidth of about 1% would be realized. Returning again to Equation 25 we can find the corresponding cavity length to be $L = 2.8 \lambda$.

We will next consider another possible limitation on cavity length: the requirement of stability with respect to single-cavity oscillation caused by beam negative conductance. Oscillation will result when the effective microwave admittance of the beam is equal to or greater than the cavity admittance.

The microwave beam admittance is given by[19].

$$\frac{G_e}{G_b} = \frac{(k_\parallel L)^2}{8\pi^4} \; \frac{V_b}{V_n} \left(1 + \frac{V_b}{V_n}\right) \left[\frac{2 - \beta_t^2}{\left(1 + \frac{V_b}{V_n}\right)^2} \; g\,(\delta k_\parallel L) + \right.$$

$$\left. k_\parallel L \beta_t^2 (1 - \beta_t^2) \frac{\Omega}{\omega} \; f\,(\delta k_\parallel L) \right] \tag{29}$$

where $G_b = I_b/V_b$ and I_b and V_b are the beam current and voltage, L is the cavity length, $k_\parallel = \omega/v_z$, $V_n = m_o c^2/e = 511$ kV, $\beta_t = v_t/c$, $\delta = (\omega - \Omega)/\omega$ and $\Omega = eB/\gamma m_o$ is the relativistic cyclotron frequency. Plots of the functions f and g are shown in Figure 22. For the condition $\omega > \Omega$, the f term has a negative peak which can result in a negative microwave beam admittance.

The cavity admittance is given by [19]

$$G_E = \left(\frac{R}{Q} Q_T\right)^{-1} \tag{30}$$

where Q_T is the total cavity Q, which in this case is given by Equation 25, and R/Q is defined by Equation 23 or by Equation 26 for long TE_{011} cavities. Also for long

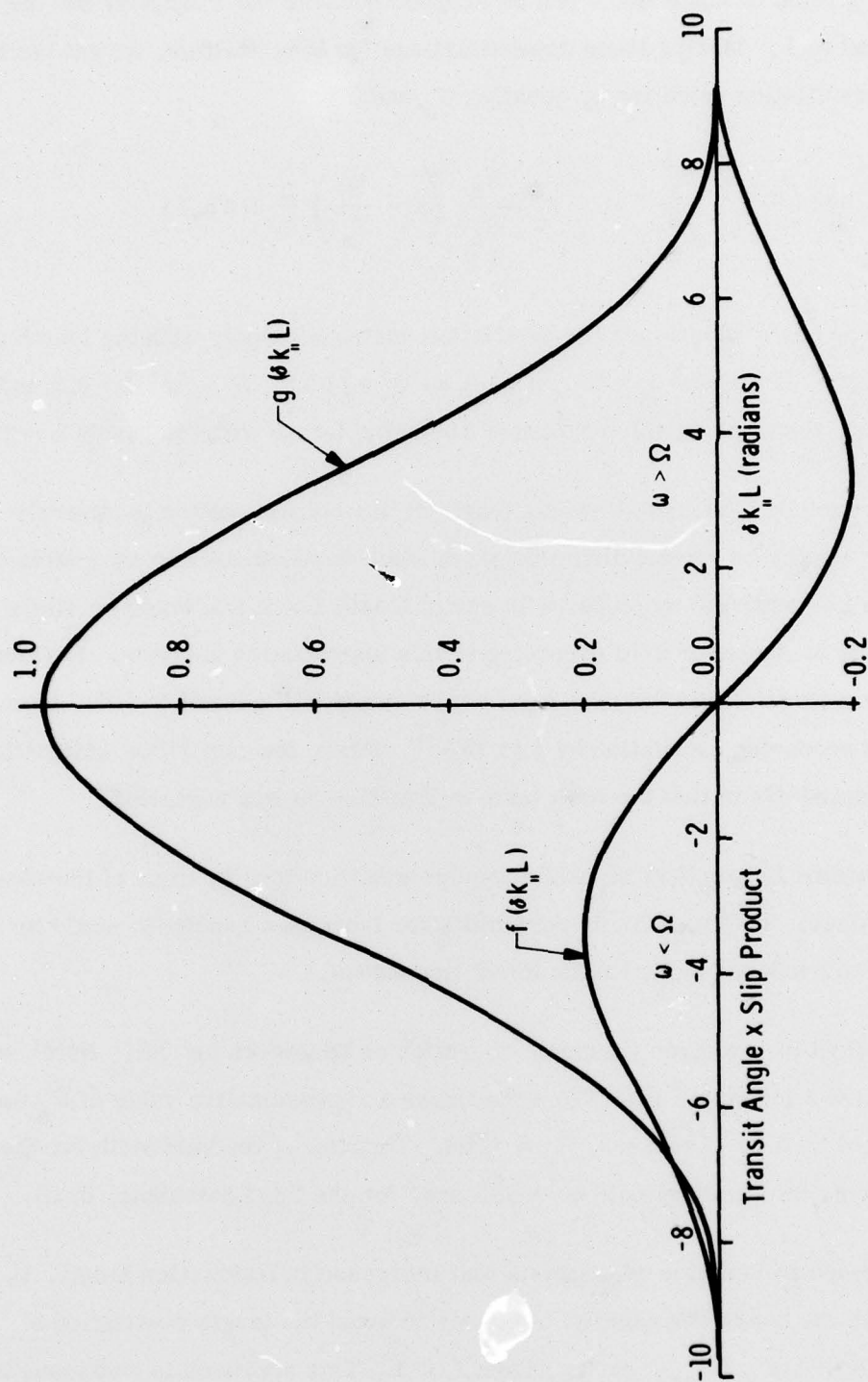Figure 22. Beam Loading Functions vs Transit Angle x Slip Product

59

cavities, the g term in Equation 29 can be dropped because the multiplier for the f term is proportional to L. Making these approximations for long cavities, we get the following start oscillation condition by equating G_e and G_E:

$$\frac{1}{G_b} = 864 \left(\frac{L}{\lambda}\right)^4 \frac{\beta_t^2}{\beta_z^3} (1 - \beta_t^2) \frac{V_b}{V_n} \left(1 + \frac{V_b}{V_n}\right) \frac{\Omega}{\omega} f(\delta k_{\parallel} L) \qquad . \qquad (31)$$

Note that the dc beam admittance for oscillation varies inversely with the fourth power of circuit length. If we take $\beta_t = 0.4$, $\beta_z = 0.2$, $V_b = 60$ kV, $\Omega \approx \omega$, $f = 0.2$ and $1/G_b = 2 \times 10^4$, then we can solve Equation 31 for the length with the result $L = 2.69 \lambda$.

It is concluded that the allowable length of any circuit section is severely limited if the conditions for maximum negative beam conductance are not avoided. For example, the 1% bandwidth amplifier with cavity length $L = 2.8 \lambda$ would oscillate over a narrow range of magnetic field according to this approximate analysis. Fortunately, however, the magnetic field for maximum power output will generally differ from the value of field producing oscillation by 5 to 10%[19]. Also, the oscillation calculation is somewhat pessimistic in that the first term in Equation 29 was neglected.

Bandwidths larger than 1% would require modifications in some of the assumed parameter values. The most likely possibility for increased bandwidth would be to develop guns to produce beams having lower impedance.

The effect of cyclotron harmonic operation on bandwidth for TE_{01} fields was shown in Figure 5 in Section III. From the figure a representative value of F_n for $n = 2$ is seen to be 0.3. For $n = 3$, $F_n \approx 0.03$. Therefore, the bandwidth for the second harmonic interaction would be 0.45% and, for the third harmonic, 0.1%.

Reference to Equation 24 suggests that increases in interaction length, L, would improve the bandwidth rapidly. One way to avoid the length restriction of Equation 25 is to use a $TE_{01\ell}$ cavity where $\ell > 1$. This approach is analagous to an extended interaction klystron. Figure 23 shows a frequency-phase diagram for this
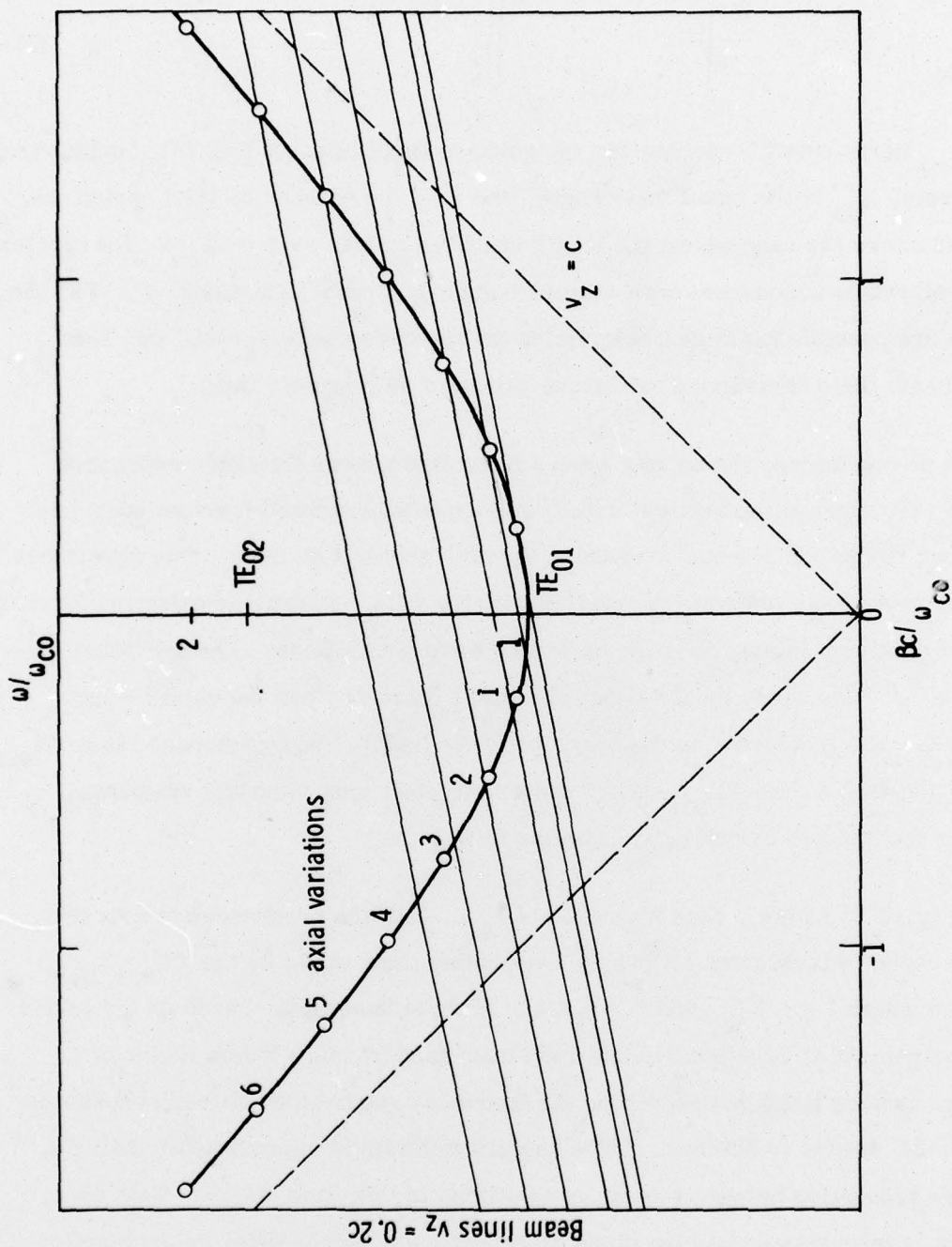
Figure 23. Phase Diagram with Cavity Length, $L = 2\lambda_{co}$ Showing $TE_{01\ell}$ Resonances

type of interaction. The parabolic curve is the characteristic curve for the cylindrical guide used to form the cavity. The allowable resonant cavity lengths are given by

$$\frac{\beta c}{\omega_{co}} = \frac{\ell \lambda_{co}}{2L} \tag{32}$$

where ω_{co} is the cutoff frequency for the guide mode of interest (the TE_{01} cylindrical in this case), λ_{co} is the cutoff wavelength, and ℓ is the number of axial variations. Figure 23 shows the case where the length has been chosen as $L = 2\lambda_{co}$. The circles indicate allowable resonances with various numbers of axial variations, ℓ. The sloping lines are possible beam characteristics for the case where $v_z = 0.2$ c. The various beam lines correspond to various values of dc magnetic field.

A strong interaction occurs when a beam line passes through a resonance point. To the right of the vertical axis are relatively broadband forward wave interactions and to the left are narrow band backward wave interactions. The uppermost beam line represents a strong interaction with the TE_{016} resonance using the forward wave and minimum interactions for backward wave oscillations. The operating frequency in that case would be 1.8 times the cutoff frequency and the cavity length would be $L = 3.6 \lambda$ where λ is the operating wave length. When compared to a TE_{011} cavity of length 3λ, the TE_{016} cavity appears to offer only a modest advantage, assuming that the two cavities have similar R/Q.

Figure 24 shows a case where $L = 4 \lambda_{co}$. Now the resonances are more closely spaced in frequency. A possible operating point would be the $TE_{0,1,10}$ resonance where $f = 1.6 f_{co}$ and $L = 6.4 \lambda$. Now the bandwidth, based on the impedance requirement of Equation 24, has been increased by more than a factor of 4. However, another limit on bandwidth, the frequency separation between resonances in Figure 24, begins to dominate. The useful bandwidth is approximately half the frequency separation between resonances, which, in this case, is 3%. This case, therefore, represents something close to the optimum for the extended interaction circuit, and one could expect a bandwidth of 3 to 4% with the assumed beam parameters.
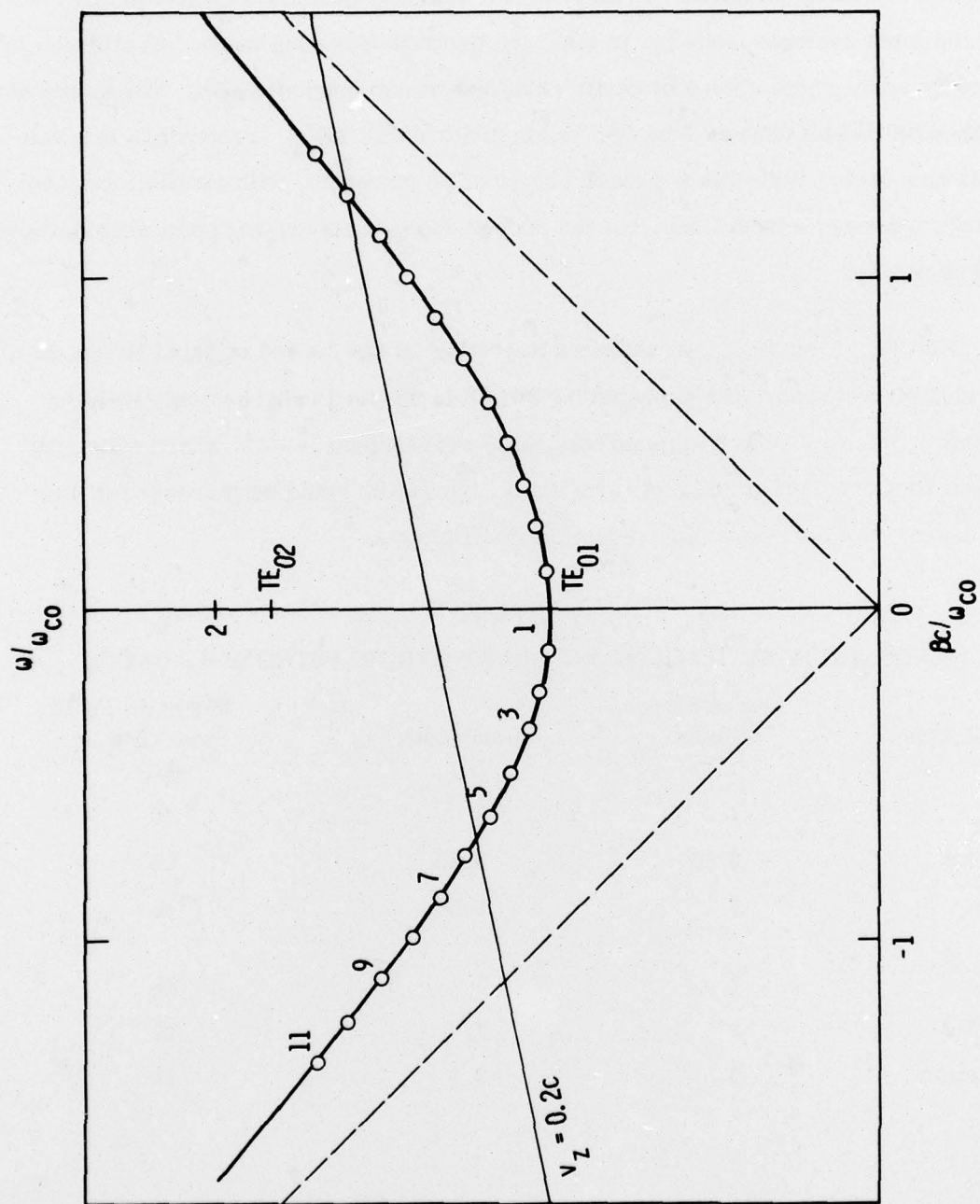
Figure 24. Phase Diagram with Cavity Length $L = 4\lambda_{co}$

In summary it is concluded that a 94 GHz amplifier having 1% bandwidth should be achievable using TE_{011} cylindrical resonant cavities operating with the fundamental cyclotron resonance condition. In this device, stability problems are minimized because the most unstable mode is, in fact, the desired operating mode. Oscillation is avoided by appropriate choice of cavity parameters and magnetic slip. For somewhat increased bandwidth such as 3 to 4%, an amplifier using $TE_{01\ell}$ resonators is a reasonable approach. With this approach one must be concerned with oscillations involving backward-wave interactions, but the proper choice of operating point should allow stable operation.

For TE_{011} or $TE_{01\ell}$ resonators operating on the second or third harmonic of the cyclotron frequency, the expected bandwidth is reduced progressively with the harmonic number. Table 3 summarizes these results for the case where efficiency has been kept constant at 30%. Alternatively, bandwidth could be increased in any given case with a corresponding reduction in efficiency.

TABLE 3.

EXPECTED BANDWIDTH OF RESONANT GYROKLYSTRONS AT 94 GHz

Circuit Type	Harmonic Number	Bandwidth (%)	Magnetic Field at 94 GHz (kg)
TE_{011}	1	1	36
Resonant	2	0.45	18
Cavity	3	0.1	12
$TE_{01\ell}$	1	3	36
Extended	2	1.4	18
Interaction	3	0.3	12

VII. CONCLUSIONS AND RECOMMENDATIONS FOR FUTURE WORK

The analysis of cyclotron harmonic interactions led to the conclusion that the strength of the interaction is strongly dependent on the position of the electron orbit centers and the specific waveguide or cavity mode being considered. It was beyond the scope of this program to do a complete evaluation of all possible modes and orbit positions. It was hoped that the limited number of calculations performed might make some general conclusions possible. However, the results appear sufficiently diverse that evaluation of more cases is needed. A tentative conclusion is that the TE_{n1} modes may be superior to the TE_{01} modes for harmonic operation and that the harmonic number need not match the angular index of the mode depending on the orbit center position.

The design, construction, and initial test of the X-band three-cavity gyro-klystron have demonstrated that this type of amplifier is feasible. This experimental vehicle represented the first known demonstration of a gyroklystron amplifier. (However, it should be noted that a two-cavity gyroklystron configuration which did not produce gain was studied earlier for somewhat different purposes[20] .) The fact that the X-band amplifier operated on the second harmonic of the cyclotron frequency is most encouraging for operation on cyclotron harmonics. Harmonic operation will allow the realization of millimeter wave amplifiers or oscillators with lower dc magnetic fields.

The measured amplifier gain of 10 dB was considerably less than the design value of 23 - 26 dB. However, interfering oscillations prevented full optimization of the beam transverse energy. Once these oscillations are eliminated, increases in gain will be possible. The oscillations that directly interfered with gain were C-band oscillations involving TE_{11} modes and the fundamental cyclotron resonance condition. To eliminate these oscillations, the TE_{11} modes must be preferentially loaded. The favored approach for loading is by axial breaks in the interaction structure loaded with lossy material.

In addition to the C-band oscillations, other X-band oscillations were observed with the magnetic fields set at values different from the design value. One of these oscillations involved the TE_{211} mode in the output cavity and produced 19.5 kw peak output at an efficiency of 9.8% at 8.330 GHz. This oscillation was an interaction at the second harmonic of the cyclotron frequency, giving further encouragement for harmonic operation.

The presence of many oscillations is, in one sense, an encouraging result since it indicates that a beam having high transverse velocity and low velocity spread was achieved. It is concluded that the capability of designing and simulating beam performance on the computer is verified to first order. However it would be useful, if not essential in the future, to develop techniques to quantitatively measure the performance of experimental beams.

From the calculations of gyroklystron bandwidth, it is concluded that a gyroklystron using TE_{011} or $TE_{01\ell}$ resonant cavities could be built with a bandwidth of 1 to 4% at 94 GHz provided a superconducting magnet is used to allow operation at the fundamental cyclotron resonance. Efficiency of such an amplifier could be 30% and power output 100 kw peak with duty factors approaching 100%. Harmonic operation, which would allow room temperature magnets, would result in significant reduction in either bandwidth or efficiency.

A traveling wave interaction using cyclotron resonance either at the fundamental or at cyclotron harmonics offers considerable promise for broader bandwidth. Both analytical and experimental work is needed for these devices. Additional work on stability is needed for the traveling wave interactions as well as the resonant devices.

66

REFERENCES

1. D. T. Swift-Hook and A. Reddish, "Cyclotron Resonance and the Generation of Millimeter Waves," Proc. Symposium on Millimeter Waves, Vol. 9, Polytechnic Institute of Brooklyn, 1959, pp 261-273.

2. K. K. Chow and R. H. Pantell, "The Cyclotron Resonance Backward Wave Oscillator," Proc. IEEE, Vol. 48, pp 1865-1870, November 1960.

3. J. L. Hirshfield and J. M. Wachtel, "Electron Cyclotron Maser," Phys. Rev. Let., Vol. 12, No. 19, pp 533-536, May 1964.

4. J. B. Bott, "A Powerful Source of Millimeter Wavelength Electromagnetic Radiation," Physics Letters, Vol. 14, No. 4, pp 293-294, February 1965.

5. J. P. Beasley, "An Electron Cyclotron Resonance Oscillator at Millimeter Wavelengths," Proc. 6th Int'l Conference on Microwave and Optical Generation and Amplification, Cambridge, pp 132-139, September 1966.

6. R. L. Schriever and C. C. Johnson, "A Rotating Beam Waveguide Oscillator," Proc. IEEE, Vol. 54, No. 12, pp 2029-2030, December 1966.

7. B. Kulke and R. W. Wilmarth, "Small Signal and Saturation Characteristics of an X-band Cyclotron-Resonance Oscillator," Proc. IEEE, Vol. 57, No. 2, pp 219-220, February 1969.

8. V. L. Granatstein, P. Sprangle, R. K. Parker, and M. Herndon, "An Electron Synchrotron Maser Based on an Intense Relativistic Electron Beam," JAP, Vol. 45, No. 5, pp 2021-2028, May 1975.

9. V. L. Granatstein, P. Sprangle, M. Herndon, R. K. Parker and S. P. Schlesinger, "Microwave Amplification with an Intense Relativistic Electron Beam," JAP, Vol. 46, No. 9, pp 3800-3805, September 1975.

10. N. I. Zaytsev, T. B. Pankratova, M. I. Petelin, and V. A. Flyagin, "Millimeter and Submillimeter Waveband Gyrotrons," Radiotekhnika i Elektronika, Vol. 19, No. 5, pp 1056-1060, 1974.

11. D. V. Kisel', G. S. Korablev, V. G. Navel'yev, M. I. Petelin, and Sh. E. Tsimring, "An Experimental Study of a Gyrotron, Operating at the Second Harmonic of the Cyclotron Frequency, with Optimized Distribution of the High Frequency Field," Radio Engineering and Electronic Physics, Vol. 19, No. 4, pp 95 - 100 (1974).

12. H. R. Jory, "Investigation of Electronic Interaction with Optical Resonators for Microwave Generation and Amplification," Final Report, Contract DA-28-043 AMC-01873(E), July 1968.

13. H. R. Jory and A. W. Trivelpiece, "Charged Particle Motion in Large Amplitude Electromagnetic Fields," JAP, 39, No. 7, pp 3053-3060, June 1968.

14. I. S. Kovalev, A. A. Kurayev, S. V. Kosolov, G. Ya. Slepyan, "The Effect of Space Charge in Gyroresonant Devices with Thin Equally Mixed and Axially Symmetrical Electron Beams," Radiotekhnika i Electronika, Vol. 19, No. 5, (1974) p 1112.

15. S. V. Kosolov, A. A. Kurayev, "Comparative Analysis of the Interaction at First and Second Harmonics of the Cyclotron Frequency in Gyroresonant Devices," Radiotekhnika i Electronika, Vol. 19, No. 10, (1974) p 2105.

16. A. L. Gol'denberg and M. I. Petelin, "The Formation of Helical Electron Beams in an Adiabatic Gun," Radio Physics and Quantum Electronics, Vol. 16, No. 1, pp 106-111, January 1973.

17. H. R. Jory, E. L. Lien, and R. S. Symons, "Final Report, Millimeter Wave Study Program," Oak Ridge National Laboratory Order No. Y-12 11Y-49438V, November 1975.

18. F. Friedlander, et al, "Development Program for a 200 kW CW, 28 GHz Gyro-klystron," Quarterly Report No. 1, Union Carbide Corp., Contract No. 53X01617C, July 1976.

19. H. R. Jory and R. S. Symons, "Supplementary Report No. 2, Millimeter Wave Study Program," prepared for Oak Ridge National Laboratory on Order No. Y-12 11Y-49438V, April 1976.

20. J. M. Wachtel and J. L. Hirshfield, "Interference Beats in Pulse-Stimulated Cyclotron Radiation," Phys. Rev. Let. 17, No. 7, pp 348-351, August 1966.

MISSION
of
Rome Air Development Center

RADC plans and conducts research, exploratory and advanced development programs in command, control, and communications (C^3) activities, and in the C^3 areas of information sciences and intelligence. The principal technical mission areas are communications, electromagnetic guidance and control, surveillance of ground and aerospace objects, intelligence data collection and handling, information system technology, ionospheric propagation, solid state sciences, microwave physics and electronic reliability, maintainability and compatibility.

AMERICAN REVOLUTION BICENTENNIAL
1776-1976